LBL-17070 c.2
UC-13

Lawrence Berkeley Laboratory

UNIVERSITY OF CALIFORNIA

RECEIVED
LAWRENCE
BERKELEY LABORATORY

JUN 12 1984

LIBRARY AND
DOCUMENTS SECTION

APPLIED SCIENCE DIVISION

FY 1983 Annual Report

CHEMICAL PROCESS RESEARCH AND DEVELOPMENT PROGRAM

April 1984

TWO-WEEK LOAN COPY

This is a Library Circulating Copy which may be borrowed for two weeks. For a personal retention copy, call Tech. Info. Division, Ext. 6782.

APPLIED SCIENCE DIVISION

LBL-17070 c.2

Prepared for the U.S. Department of Energy under Contract DE-AC03-76SF00098

DISCLAIMER

This document was prepared as an account of work sponsored by the United States Government. While this document is believed to contain correct information, neither the United States Government nor any agency thereof, nor the Regents of the University of California, nor any of their employees, makes any warranty, express or implied, or assumes any legal responsibility for the accuracy, completeness, or usefulness of any information, apparatus, product, or process disclosed, or represents that its use would not infringe privately owned rights. Reference herein to any specific commercial product, process, or service by its trade name, trademark, manufacturer, or otherwise, does not necessarily constitute or imply its endorsement, recommendation, or favoring by the United States Government or any agency thereof, or the Regents of the University of California. The views and opinions of authors expressed herein do not necessarily state or reflect those of the United States Government or any agency thereof or the Regents of the University of California.

LBL-17070

APPLIED SCIENCE DIVISION ANNUAL REPORT

CHEMICAL PROCESS RESEARCH & DEVELOPMENT PROGRAM

FY 1983

Elton J. Cairns
Program Leader
Head, Applied Science Division
and
Associate Director, LBL

Report Coordinator
Maya Osowitt

Applied Science Division
Lawrence Berkeley Laboratory
University of California
Berkeley, California 94720

Prepared for the U.S. Department of Energy under Contract No. DE-AC03-76SF00098

CONTENTS

Chemical Process Research and Development Program Staff 1-v

Introduction 1-1

FUELS FROM BIOMASS BY BIOCHEMICAL PROCESSES

High-Productivity Vacuum Fermentation Processes
B.L. Maiorella, H.W. Blanch, and C.R. Wilke 1-2

Bioconversion of Cellulose: Enhanced Cellulase Production Using Solka Floc in a Fed-Batch Fermentation
H.Blanch, C. Wilke, P. Cevey, N. Hendy, and A. Joglekar 1-5

ORGANOMETALLIC GEOCHEMISTRY

Synthesis of an Encapsulated Arsenic Anion via Reaction of Arsenic Acid with a Linear Catecholamide, 3,4-LICAM
R.H. Fish and R.S. Tannous 1-9

Molecular Characterization of Vanadyl and Nickel Porphyrin and Non-porphyrin Compounds in Heavy Crude Petroleums and their Asphaltines
R.H. Fish, J.J. Komlenic, and B.K. Wines 1-11

Homogeneous Catalytic Hydrogenation: Selective Reductions of Polynuclear Heteroaromatic Compounds Catalyzed by Chloro(Tristriphenylphosphine)Rhodium(I)
R.H.Fish, A.D. Thormodsen, and H. Heinemann 1-20

A Comparison of Polymer-Supported Wilkinson's Catalyst with its Homogeneous Analogue in the Selective Reduction of Polynuclear Heteroaromatic Compounds
R.H. Fish, A.D. Thormodsen, and H. Heinemann 1-25

COAL-RELATED RESEARCH

Processing of Condensate Waters from Coal Gasification
C.J. King, D. Mohr, P. MacKenzie, J. Senetar, J. Bixby, R. Demyanovich, and R. Thompson 1-29

Enhancing Efficiency in Dry-Ash Moving-Bed Gasifiers Through a Distributed Feed
C.H. Lu and M.M. Dean 1-34

ELECTROCHEMICAL ENERGY STORAGE RESEARCH

Technology Base Research Project for Electrochemical Energy Storage
E.J. Cairns, K. Kinoshita, and F.R. McLarnon 1-39

Battery Electrode Studies
E.J. Cairns, F.R. McLarnon, J.C. Dobson, J.H. Flatt, R.I. Goldberg, M. Isaacson, R. Jain, P.M. Lessner, K.G. Miller, M.L. Smith, and K.A. Striebel 1-41

ADVANCED THERMAL ENERGY STORAGE RESEARCH

Advanced Thermal Energy Storage Technologies
P. Berdahl, A. Hunt, C. Tien, and R.J. Otto 1-46

CHEMICAL PROCESS RESEARCH AND DEVELOPMENT PROGRAM STAFF

Elton Cairns, Program Leader
Harvey Blanch, Deputy Program Leader

Myra Baker
James Bixby
Douglas Bousfield
Garth Burns
Robert Chung
Robert Demyanovich
Morton Denn
Jesse Dobson
Gregory Dow
Betsy Elzufon
Richard Fish
James Flatt
Raymond Gansley
Robert Goldberg
Edward Grens
Donald Hanson
Mark Isaacson
Rajiv Jain
Eileen Keefe
C. Judson King
John Komlenic
Phillip Lessner
Gary Lipscomb
Scott Lynn
Patricia MacKenzie
Frank McLarnon
Brian Maiorella
Anthony Mancusco
Kenneth Miller
Donald Mohr
Robert Moore
Curtis Munson
Thomas Murphy
Timothy Oolman
Michael Pedersen
Aldo Sciamanna
John Senetar
Jon Sindquist
Michael Smith
Kathy Streibel
Raja Tannous
Rodney Thompson
Arne Thormodsen
Theodore Vermeulen*
Bruce Vickroy
James Walter
David Watt
Dale Wiley
Charles Wilke
Brian Wines
Harry Wong

*Deceased October 28, 1983.

CHEMICAL PROCESS RESEARCH AND DEVELOPMENT PROGRAM

INTRODUCTION

The Chemical Process Research and Development Program has five main projects applying chemistry and chemical engineering to problems in the production of unconventional new fuels, their environmental impact, and energy storage. These projects are:

(a) Reaction engineering of coal gasification and liquefaction
(b) Processing of effluent gases and liquids resulting from such synthetic-fuel production, to provide acceptable waste or recycle streams
(c) Production of liquid fuels from biomass
(d) Electrochemical energy storage
(e) Thermal energy storage.

Each of these projects focuses on transport-process principles, chemical kinetics, thermodynamics, separation processes, and organic and physical chemistry.

The first project has three aspects. The first involves an analysis of the moving-bed coal gasifier. The effect of feed configuration on the efficiency of the dry-ash gasifier is being examined by developing models for simulating the process. The second aspect involves the removal of metal compounds from the complex chemical matrices that make up fossil-fuel precursors and products. Such removal is important for efficient refining and for environmental protection. Accordingly, LBL has developed a program to molecularly characterize these organometallic and inorganic complexes. The program is also developing innovative methods to remove these compounds by using model ligands for future polymer-supported analogues. The third aspect concerns basic research in coal liquefaction. The emphasis is on ways to selectively hydrogenate model coal compounds. This would provide an immense saving in hydrogen gas and new process technology for the petroleum industry, as well as an advance in our knowledge of reaction mechanisms.

The second project involves the development of novel and improved methods for processing synfuel condensate waters to make them suitable for recycle, thereby minimizing process-water requirements. The main emphasis is on physiochemical methods, particularly solvent extraction and stripping, to remove organics. Identification of the contaminating organics is difficult, but necessary to permit development of appropriate solvents for their removal. LBL studies have successfully examined simultaneous solvent extraction in removal of ammonia and acid gases by stripping.

The conversion of biomass to liquid fuels has been an area of considerable research and development within the Chemical Process Program over the past several years. The biological conversion of wood and agricultural residues to ethanol has been examined. An enzymatic hydrolysis of these cellulosic materials has been developed to yield monomeric hexose and pentose sugars. These can be subsequently fermented to produce ethanol. Various high-rate fermentation processes have been developed, and novel processes for ethanol recovery that are less energy intensive than conventional processes are being studied.

The electrochemical energy storage program provides research to develop advanced battery systems for electric vehicle and stationary energy storage applications. Topics include identification of new electrochemical couples for advanced batteries, determination of technical feasibility of the new couples, improvements in battery components and materials, establishment of engineering principles applicable to electrochemical energy storage and conversion, and the assessment of fuel-cell technology for transportation. Major emphasis is on applied research that will lead to superior performance and lower life-cycle costs.

A fifth project was added late in FY 1983. This is a series of research and development efforts in thermal energy storage. The project will focus on new and innovative approaches with a broad range of applications and the utilization of solar energy.

FUELS FROM BIOMASS BY BIOCHEMICAL PROCESSES

High-Productivity Vacuum Fermentation Processes*

B.L. Maiorella, H.W. Blanch, and C.R. Wilke

The research of the Biochemical Processes Group has focused on the hydrolysis of lignocellulosic materials to sugars and their subsequent fermentation by yeast to ethanol and other fuel-grade chemicals. Various studies have examined the kinetics of enzymatic hydrolysis of cellulose and hemicellulose fractions for optimal sugar production, the physical and chemical nature of the raw materials, the optimal production and recovery of enzymes, and the use of new organisms for converting polymeric pentosans and hexosans to sugars. Optimization of the continuous ethanol removal and recovery process, as well as alternative methods of fermentation to ethanol, has also been studied. In all this work, the economic impact of any change in a process is evaluated.

In this article, we report on efforts to improve the ethanol yield of vacuum fermentation processes.

ACCOMPLISHMENTS DURING FY 1983

The Vacuferm Process

The vacuferm process (Fig. 1) was developed concurrently by Cysewski and Wilke[1] and by Ramalingham and Finn.[2] The fermentation vessels are operated under vacuum (approximately 75 mmHg absolute pressure), and ethanol is boiled away at 35°C as it is produced. By controlling the pressure, the residual equilibrium ethanol concentration in the fermentor beer can be regulated at levels tolerable to the yeast (less than about 87 g/L) while still allowing the fermentation of very concentrated sugar solutions (up to 50 wt% glucose). The flashing within the fermentors is a single-stage distillation in which most of the ethanol product can be removed as a concentrated vapor. A small portion of the beer is taken as a liquid bleed to purge the system of nonvolatile components. This bleed stream contains the by-product yeast. After stripping for residual ethanol recovery, the remaining yeast solids are dried as a cattle feed supplement.

The ethanol/water-vapor equilibrium mixture (along with noncondensible CO_2 and O_2 gases) is drawn from the fermentors through large vacuum compressors.

Vapor recompression heating provides energy for boilup in the fermentor, resulting in substantial energy savings. Rather than compressing the overhead vapor entirely to atmospheric pressure, the main compressor compresses the vapor to only about 350 mmHg. At this pressure, the vapor dew point is raised, and the vapor can be condensed in the fermentor reboiler to provide heat for further boilup. The condensed clean liquid can then be pumped with very little energy to distillation column pressure. A second compressor compresses the noncondensible CO_2 and O_2 gases (along with the equilibrium residual ethanol and water) to atmospheric pressure. Further liquid is condensed, and the noncondensibles are purged.

Vacuum fermentation and vacuum distillation combine synergistically,[1] and the energy-saving vacuum distillation is used for the final ethanol purification step. The vacuum flashing generally produces a sufficiently concentrated ethanol feed for efficient distillation. For very dilute fermentor beers, supplementary stripping with vapor heat may be required to maintain the energy efficiency of distillation.[3]

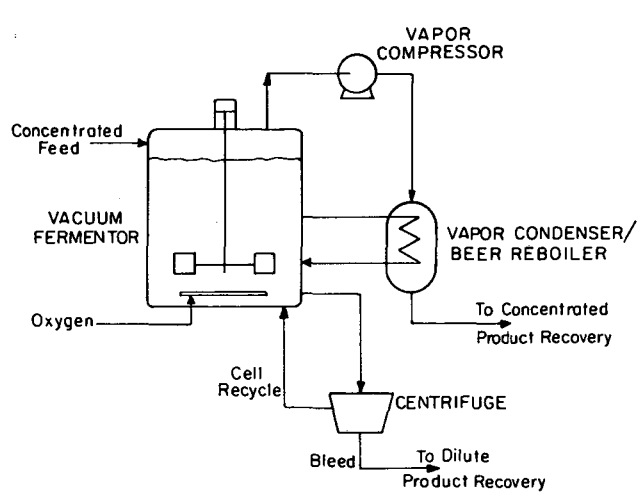

Figure 1. Vacuum fermentation. (XBL 836-5899)

*This work was supported by the Assistant Secretary for Conservation and Solar Energy of the U.S. Department of Energy under Contract No. DE-AC03-76SF0098 and by the Solar Energy Research Institute under Contract No. DR-0-9058-1.

Although the simple vacuferm process allows rapid fermentation of concentrated feeds to a concentrated product with a considerable reduction in the size of the fermentation and auxiliary equipment, many aspects of the design could potentially be improved. Oxygen solubility in the beer is greatly reduced under vacuum, and to meet the oxygen requirements of the yeast, costly pure oxygen must be sparged into the fermentor.[1] Noncondensible carbon dioxide gas is produced in equimolar proportion with ethanol. All of the CO_2 gas must be purged from the vacuum fermentors through the compressors. The compressor size and energy requirements are thus much larger than if only the equilibrium ethanol/water-vapor product was compressed.

Ethanol is recovered from the compressed gas stream by condensing in the fermentor reboiler and auxiliary exchangers. Noncondensible CO_2 and O_2 gases interfere with condensation, decreasing effective heat transfer coefficients and increasing the required heat exchanger surface area. Finally, the high CO_2 concentrations at the elevated compressor discharge temperatures increase corrosion rates.

The Flashferm Process

The flash fermentation or flashferm process (Fig. 2), originally proposed conceptually by Wilke,[4] makes several improvements on the vacuferm process. Fermentation is carried out in atmospheric pressure fermentors. The yeast oxygen maintenance requirement can be met with inexpensive air sparging. Carbon dioxide is evolved and vented directly from the fermentor (with no compression required). To remove ethanol as it is produced, the fermenting beer is rapidly cycled from the fermentor through a vacuum flash expansion vessel (FEV), where the ethanol is boiled away. A concentrated vapor product is taken overhead from the flash vessel, and ethanol-depleted beer is recycled to the fermentor for further conversion. Only the small amount of CO_2 dissolved in the beer must be processed through the compressor. This consists of CO_2 carried into the flash vessel and CO_2 generated by fermentation during the short residence time in the flash vessel. Thus, compressor capacities can be reduced, improving the heat transfer coefficients in the vapor condensers and reducing the exchanger area. The large vacuferm product absorber can be eliminated entirely.

For improved efficiency, the flash vessel temperature can be slightly lower than the fermentor temperature so that returning liquid will provide the required fermentor cooling. The microbial heat of reaction (117 kcal/kg glucose consumed[5]) is thus

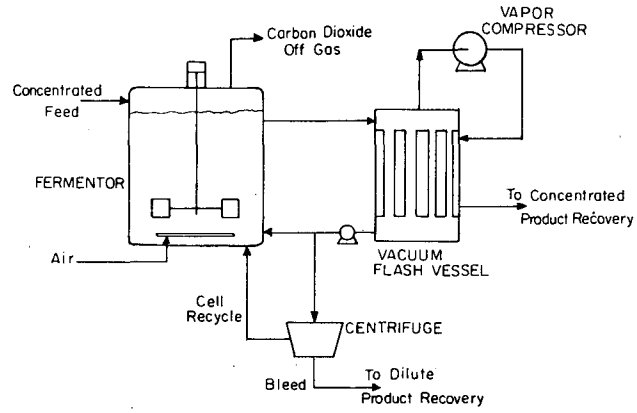

Figure 2. Flash fermentation. (XBL 836–5898)

recovered to help vaporize the ethanol product in the flash vessel. The flash vapors, after compression, generally contain excess superheat so that complete recovery of the microbial heat for flashing is not necessary. A flash vessel temperature between 2 to 3 degrees below the fermentor temperature results in a balance so that additional fermentor cooling is not required. This small temperature reduction does not adversely affect the yeast, but the flash pressure is reduced, increasing the compressor cost. This design, by not requiring an exact heat balance, but instead allowing supplementary cooling of the fermentors by submerged cooling coils, offers control advantages by partially decoupling the flash vessel and fermentor operations.

At the low pressure required for ethanol flashing, the specific volume of the ethanol/water vapor is very large, so that (as with the vacuferm process) extremely large compressors are needed. Although the horsepower requirements are modest, these large vacuum compressors are very costly.[6]

The Frigferm Process

Refrigerative flash fermentation, or frigferm (Fig. 3), is a further modification of the simple flashferm process and is intended to reduce capital costs by reducing the vacuum compressor size. An external-loop heat pump is used. Cold refrigerant is evaporated in the flash vessel and most of the resulting ethanol/water vapors are condensed by an overhead condenser. Heat for boilup is recovered by recondensing the refrigerant in heat exchange with the flash-vessel liquid. The condensed ethanol/water liquid is pumped to distillation-column pressure. Now, only a small fraction of the original vapor remains to be compressed from the flash-vessel pressure to atmospheric pressure, so a small compressor can be used. A second refrigeration system is

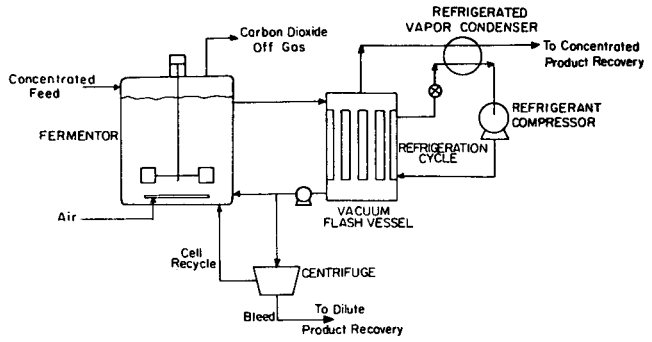

Figure 3. Refrigerative flash fermentation.
(XBL 836-5900)

required, but the refrigerant compressors are of ordinary physical dimensions (and more modest cost), because they are compressing a refrigerant of much lower specific volume than ethanol/water vapor at low pressure.[7]

Conclusions

Table 1 summarizes results for the optimized vacuferm, flashferm, and frigferm designs and compares these with the batch process and the optimized conventional design that uses continuously stirred tank fermentors with cell recycle (CSTR). Both flash and refrigerative flash fermentation achieve substantial capital investment and manufacturing cost savings compared to the CSTR. These savings are directly offset, though, by the reduction in yeast byproduct credits owing to the reduction in yeast growth caused by secondary product and feed component inhibition. Overall, no savings are achieved. Compressor systems for all vacuum fermentation schemes are very costly, and alternative ethanol removal methods (such as extraction) may be more attractive.

PLANNED ACTIVITIES FOR FY 1984

The use of flash fermentation with ethanol-inhibited thermophilic organisms is quite promising. To use xylose-fermenting *Clostridia*, for example, conditions of 65°C and 4.5 wt% ethanol concentration are anticipated. If we take the standard byproduct credits and set a 15% simple return on investment (excluding the cost of xylose feed, which is not yet known), the ethanol product cost is reduced 39%, from 21.2¢/L to 13.0¢/L. Further work on this approach is clearly warranted, and is one of the activities continuing into FY 1984.

REFERENCES

1. Cysewski, G.R., and Wilke, C.R. (1978), "Process Design and Economic Studies of Alternative Fermentation Method for Production of Ethanol," *Biotechnol. Bioeng. 20,* p. 1421.
2. Ramalingham, A., and Finn, R.K. (1977), "The Vacuferm Process; A New Approach to Fermentation of Alcohol," *Biotechnol. Bioeng. 19,* p. 583.
3. Maiorella, B.L. (1983), "Vacuum Ethanol Distillation Technology," in *The Ethanol Separation Handbook*, L. Douglas, ed., Solar Energy Research Institute, Golden, Colorado.
4. Wilke, C.R. (1977), personal communication with G. Cysewski.

Table 1. Cost comparison of fermentation processes.

	Purchased Equipment Cost						
Process	Storage ($\$10^5$)	Fermentation ($\$10^5$)	Ethanol + Stillage Recovery ($\$10^5$)	Total ($\$10^5$)	Manufacturing Cost (¢/L)	Yeast Credit (¢/L)	Final Product Cost (¢/L)
Batch	6.90	18.01	33.86	58.77	10.9	4.8	53.05
Recycle CSTR	6.90	11.31	30.21	48.42	8.64	4.8	49.06
Vacuferm	7.11	27.22	16.93	51.25	6.85	2.1	51.48
Flashferm	6.92	26.66	12.70	46.28	6.20	1.7	49.44
Frigferm	6.92	22.19	12.69	41.80	5.93	1.7	48.51

5. Lamprecht, I., and Meggers, C. (1969), "Microcalorimetric Study on the Effect of Stirring on the Growth of Yeast," *Z. Naturforsch 246*, p. 1205.
6. Bertoli, J., and Martin, W.F., design quotation by Allis Chalmers Co. for Lawrence Berkeley Laboratory, October 9, 1980.
7. Morphis, J., design quotation by Penjerdel Refrigerator Co. for Lawrence Berkeley Laboratory, November 21, 1980.

Bioconversion of Cellulose: Enhanced Cellulase Production Using Solka Floc in a Fed-Batch Fermentation*

H. Blanch, C. Wilke, P. Cevey, N. Hendy, and A. Joglekar

Perhaps the most obvious area for improvement in the process of cellulose utilization is the production of cellulase enzyme for hydrolysis of wood and agricultural residues. It has been estimated that enzyme production alone accounts for some 50% of the cost of producing glucose from cellulosic material.[1] Improvements in enzyme production would therefore have a dramatic impact and are of paramount importance if economical hydrolysis processes are to be realized. The first major step in this direction has been the development of mutant strains of the fungus *Trichoderma reesei* that are free of catabolite repression and capable of constitutive cellulase production.[2,3]

While further high-yielding mutants continue to be developed, improvements must also be made in fermentation techniques. A major advance is the use of fed-batch cultivation, which avoids the agitation and aeration difficulties, as well as the repression effects, of batch fermentation with highly concentrated substrate. This report briefly compares batch and fed-batch operations over a range of substrate concentrations.

ACCOMPLISHMENTS IN FY 1983

Much research effort has focused on the optimization of fermentor parameters for maximum enzyme yield and productivity. With high yields and high productivity, the cost of enzyme involved in the conversion of cellulosic materials to ethanol can be reduced. By increasing cellulose concentration, controlling the temperature and pH, and using resistant cellulose such as cotton milled through double rollers enzyme yields can be increased. Beyond a 6–8% increase in cellulose concentration, however, there is no proportional increase in cellulase.

Increasing the cellulose concentration also increases the bulk density and viscosity of the broth, limiting the oxygen supply to the organism. This prevents the organism from metabolizing the reducing sugar produced by cellulose degradation, which in turn represses the production of enzyme. This difficulty can be solved by carrying out fermentation under either continuous or fed-batch cultivation (slow feeding of cellulose). Either method overcomes the problems of repression and oxygen limitation, thereby increasing the enzyme yield and productivity. We carried out experiments with fed-batch cultivation to examine the effect of plant growth regulators on enzyme production and the effect of pH and temperature on enzyme activity and productivity.

The organism used was *Trichoderma reesei* Rut-C30,[2] and the cellulose substrate was Solka Floc BW200 (Brown Company, Berlin, NH). The medium was similar to the standard salt medium for *T. reesei*,[4] with increased levels of all nutrients at high cellulose concentrations. Cultivation was carried out in a New Brunswick Mini-Ferm (5 liters) at an operating volume of 2.5 liters. Nitrogen was supplied by adding ammonium hydroxide and maintaining the pH at 5.0; the temperature was controlled at 28°C.

Filter paper activities are expressed as International Units/mL, and were assayed according to Mandels *et al.*[5] β-glucosidase activity was determined by glucose released (measured by an Instruments Laboratory Glucose Analyzer) from cellobiose, and is expressed as IU/mL. Soluble protein was measured by the Lowry method.[6]

Initial experiments were carried out in shake flasks to optimize the concentration of plant growth regulators used to increase enzyme yield. The results indicated that the plant growth regulators at greater than 10^{-1} molar concentration in the medium inhibited growth and enzyme production. Molar concentrations of 10^{-6} to 10^{-8} showed marginal increases

*This work was supported by the Assistant Secretary for Conservation and Solar Energy of the U.S. Department of Energy under Contract No. DE-AC03-76SF00098 and by the Solar Energy Research Institute under Contract No. DR-0-9058-1.

in activity and no effect on the growth of the organism.

Additional plant growth regulator in the fed-batch system at 10^{-5} molar concentration showed promising results—a 12% increase in filter paper activity, a 28% increase in carboxymethyl cellulase activity, and a 50% increase in β-glucosidase activity, with no effect on cotton activity. The total addition of cellulose (about 15%) resulted in no further increase in activity, perhaps because of the lack of sufficient salts or trace elements. This was confirmed by the addition of corn-steep liquor, which resulted in an increase in enzyme production.

To make the production of enzyme still more economical, experiments were carried out with cell recycle, and these showed very high productivity and activity at 48–72 hours. But after 120–144 hours, there was no further increase in the enzyme activity.

Three pH conditions were examined for the fed-batch system: (1) pH 5.0 throughout the fermentation period; (2) pH 6.0 for the first 24 hours and pH 5.0 thereafter, as this had increased enzyme yield in a batch system; and (3) pH 4.0 throughout the fermentation. Results showed that pH 5.0 is the best for enzyme production. These experiments were carried out at 28°C. Additional experiments are needed to study in greater detail the effect of pH on enzyme production.

Experiments were also carried out to find the optimum temperature for productivity and growth rates. The pH was maintained at 5.0. The temperature was maintained at 30°C for the first 24 hours and then lowered to 28°C. At the same time, pelletized cellulose was added. The higher temperature for a short time, especially in the beginning, helped to increase the growth rate and the enzyme yield. Further experiments are required to determine the effect of temperature on enzyme activity and productivity.

These experiments have given indications on how to improve the yield. Improvements may come from more closely monitoring the flow rate of cellulose, or by intermittently adding salts and by studying in detail fermentor parameters such as temperature and dissolved oxygen. All of these parameters play a major role in enzyme production.

With conventional batch culture techniques, it has been reported,[7–9] and confirmed in this work, that, above approximately 50 g/L, increasing the concentration of Solka Floc substitute does not lead to a proportional increase in cellulase activity. This is demonstrated in Fig. 1 for concentrations of 20, 50, 75, and 100 g/L Solka Floc. The high substrate levels result in high cell mass production (accompanied by agitation and aeration difficulties), extended fermentation times, and, consequently, reduced productivity.

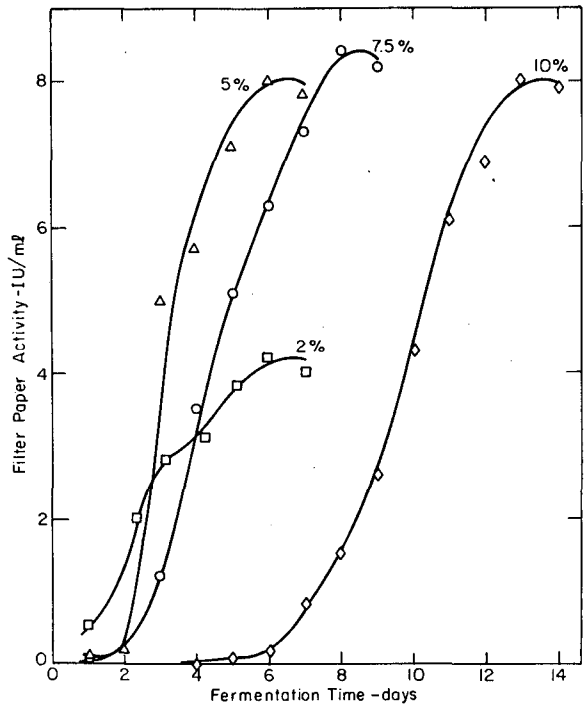

Figure 1. Batch growth of *T. reesei*, Rut-C30, with varying levels of Solka Floc. (XBL 829–6510)

In the fed-batch experiments, fermentation was initiated with a conventional batch (up to 48 hours), using 20 g/L Solka Floc as the initial concentration. After 48 hours, more Solka Floc was added to raise the substrate level to more than 20 g/L. This addition was repeated at 10- to 20-hour intervals, whenever the growth was observed to be decreasing as demonstrated by a decreasing base addition rate. In this manner, the total effective Solka Floc concentration was raised to as high as 150 g/L.

As shown in Fig. 2, this resulted in a proportional increase in cellulase production, up to the limit of cellulose concentration used in this work. A maximum of 30.4 filter paper IU/mL was achieved (the highest activity yet reported for this strain), with 47.6 g/L soluble protein. In each case, β-glucosidase activity increased similarly, reaching approximately 8.7–9.8 IU for each unit of filter paper activity. The high titer productivity (activity/mL) and maximum productivity (IU/L-hrs) of filter paper activity for both batch and fed-batch operation are shown in Table 1.

The major benefit of fed-batch operation is the ability to achieve both high enzyme titer and high productivity concurrently. High productivity has

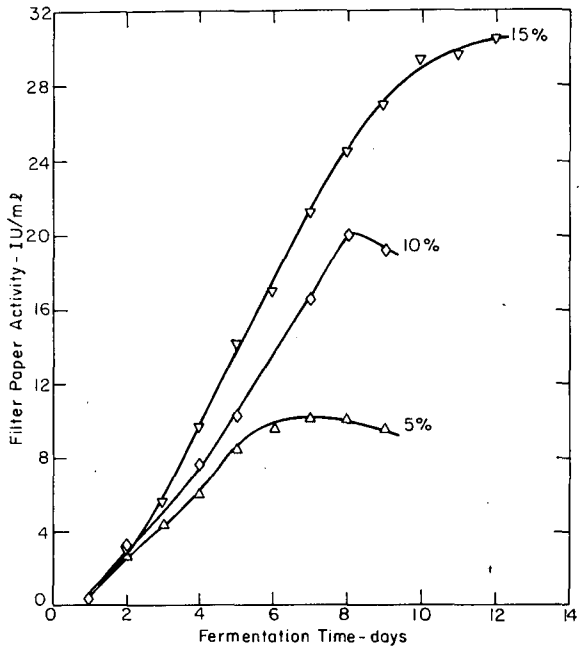

Figure 2. Fed-batch growth of *T. reesei*, Rut-C30, on Solka Floc with intermittant dosage feeding to equivalent final levels. (XBL 829-6511)

been achieved previously by continuous cultivation[9,10] and by immobilized cells,[11] but these high productivities are gained at the cost of relatively low enzyme activity per milliliter. Gottvaldova *et al.*[12] recently utilized fed-batch operation at low substrate levels (up to 45 g/L) to demonstrate increased productivity (at fairly low titer) over batch growth. However, the major advantage of fed-batch cultivation is the opportunity to use very high substrate levels, and so gain high productivity at correspondingly high enzyme titers.

Another advantage is reduced production of cell mass. The mycelium does not attain the high density found during high substrate batch growth. This ensures adequate agitation and aeration with lower power input.

PLANNED ACTIVITIES FOR FY 1984

The results reported here suggest that further effort should be on fed-batch processes as an effective method of cellulase production, and such an effort is planned for FY 1984, utilizing relatively more economical steam-exploded wood.

REFERENCES

1. Perez, J., Wilke, C.R., and Blanch, H.W. (1980), "Economics of Sugar Production with *Trichoderma reesei,* Rutgers C-30 Strain," LBL-11489.
2. Montenecourt, B.S. and Eveleigh, D.E. (1977), "Preparation of Mutants of *Trichoderma reesei* with Enhanced Cellulase Production," *Appl. Environ. Microbiol. 34*, p. 777.
3. Gallo, B.J., "Production and Characterization of Cellulolytic Enzymes" (paper 39c), presented at the American Institute of Chemical Engineers (AIChE) Winter Meeting, Orlando, FL, February 1982.
4. Mandels, M., and Reese, E.T. (1957), "Induction of Cellulase in *Trichoderma viride* as Influenced by Carbon Sources and Metals," *J. Bacteriol. 73*, p. 269.
5. Mandels, M., Andreotti, R., and Roche, C. (1976), "Measurement of Saccharifying Cellulase," *Biotechnol. Bioeng. Symp. 6,* p. 21.

Table 1. Cellulase activities produced by batch and fed-batch fermentation over a range of substrate concentrations.

	Solka Floc concentrations (g/L)	Filter paper activity (IU/mL)	Productivity	
			High titer (IU/L-hr)	Maximum (IU/L-hr)
Batch	20	4.2	29	46
	50	8.0	55	140
	75	8.4	44	83
	100	8.0	26	73
Fed-batch	50	10.0	60	93
	100	20.0	104	136
	150	30.4	106	177

6. Lowry, O.H., Rosebrough, N.J., Farr, A.L. and Randall, R.J. (1951), "Protein Measurement with the Folin Phenol Reagent," *J. Biol. Chem. 193*, p. 265.

7. Sternberg, D. (1976), "A Method for Increasing Cellulase Production by *Trichoderma viride,*" *Biotechnol. Bioeng. 18,* p. 171.

8. Sternberg, D., and Dorval, S. (1979), "Cellulase Production and Ammonia Metabolism in *Trichoderma reesei* on High Levels of Cellulose," *Biotechnol. Bioeng. 21,* p. 181.

9. Ghose, T.K., and Sahai, V. (1979), "Production of Cellulases by *Trichoderma reesei*, QM-9414 Strain, in Fed Batch and Continuous Flow Culture with Cell Recycle," *Biotechnol. Bioeng. 21,* p. 283.

10. Ryu, D., *et al.* (1979), "Studies on Quantitative Physiology of *Trichoderma reesei* with Two State Continuous Culture for Cellulase Production," *Biotechnol. Bioeng. 21,* p. 1887.

11. Montenecourt, B.S., *et al.* (1982), "Production and Characterization of Cellulolytic Enzymes" (paper 39b), presented at the AIChE Winter Meeting, Orlando, FL, February 1982.

12. Gottvaldova, M., Kucera, J., and Podrazky, V. (1982), "Enhancement of Cellulase Production by *Trichoderma reesei* using Cellulose and Ammonia in Double Fed Batch," *Biotechnol. Lett. 4,* p. 229.

ORGANOMETALLIC GEOCHEMISTRY

Synthesis of an Encapsulated Arsenic Anion via Reaction of Arsenic Acid with the Linear Catecholamide 3,4-LICAM*

R.H. Fish and R.S. Tannous

The molecular characterization of inorganic and organometallic compounds present in fossil-fuel precursors and their products has become increasingly important as our synthetic fuel industry develops. These compounds are thought to be responsible for the poisoning of process catalysts and their presumed effects on man and his environment.[1]

We have recently characterized inorganic arsenic and organoarsenic compounds in oil shale,[2] shale oil,[3] and oil shale retort waters,[4] and have proved that arsenate (AsO_4^{-3}), **1**, and methyl- and phenylarsonic acids, **2** and **3**, are present.

Although the molecular characterization of these arsenic compounds is an important first step in understanding their biogeochemical origin and their presence in fossil-fuel products, their removal from these complex matrices, using innovative methods, remains a primary goal of our program. In this regard, we recently reported on a novel method that used substituted catechols as models compounds **2** and **3**.[5]

Similar reactions with **1** have focused on a class of linear catecholamide compounds (LICAM) synthesized by Raymond *et al.*[6–14] to be used eventually for the removal of iron and actinide metal ions in clinical applications. We were particularly interested in 3,4-LICAM, **4**,[7] a ligand with three catechols on a linear amide chain. This compound could potentially coordinate in an octahedral configuration around an arsenic anion and be placed in a polymeric backbone for removal of **1** from complex matrices.

In this report, we wish to demonstrate that the reaction of 3,4-LICAM, **4**, with **1** provides a novel encapsulated arsenic anion, **5** (X = H), as shown in Eq. (1):

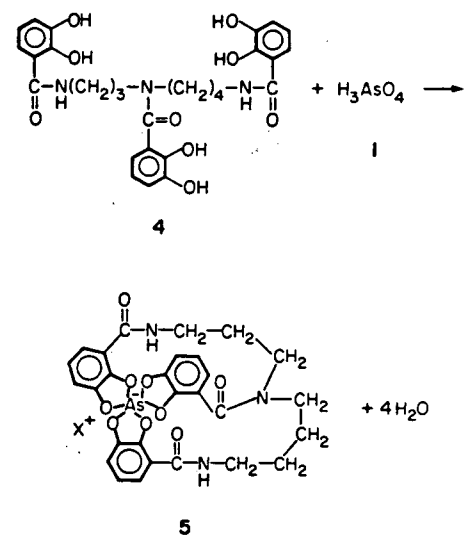

(1)

ACCOMPLISHMENTS DURING FY 1983

The ligand, **4**, reacted with **1** in an aqueous ethanol solution and, after work-up, gave a white powder (83%) that decomposed at 275–276°C. The material was analyzed spectroscopically by carbon-13 nuclear magnetic resonance (NMR), infrared, ultraviolet, and fast-atom bombardment mass spectroscopy (FAB-MS) techniques, as well as by elemental analysis. These studies provided evidence for the structure designated **5** (X = H) in Eq. (1). A tetraammonium salt (X = benzyldimethylphenylammonium) and the PPN salt were also prepared; unfortunately, they were found to be unsuitable for single-crystal x-ray studies.

The ^{13}C NMR spectrum of the acid (X = H), **5**, is shown in Fig. 1 along with that of the ligand, **4**; clearly, the arsenic anion has the simpler spectrum. The carbonyl region, ~160–170 ppm, should contain three carbonyl resonances; however, **4** has more carbonyl lines (about six to eight), indicative of a possible role of geometrical isomers (syn- and anti-isomers with eight possible carbonyl resonances). Thus, upon arsenic coordination, the carbonyl region is somewhat simplified (three or four carbonyls) with resonances at 163.6, 164 (shoulder), 168, and 169.6 ppm. The aromatic carbons with hydroxyl groups in

*This work was supported by the Assistant Secretary for Fossil Energy and the Division of Oil, Gas, and Shale Technology of the U.S. Department of Energy through the Bartlesville Energy Technology Center under Contract No. DE-AC03-76SF00098.

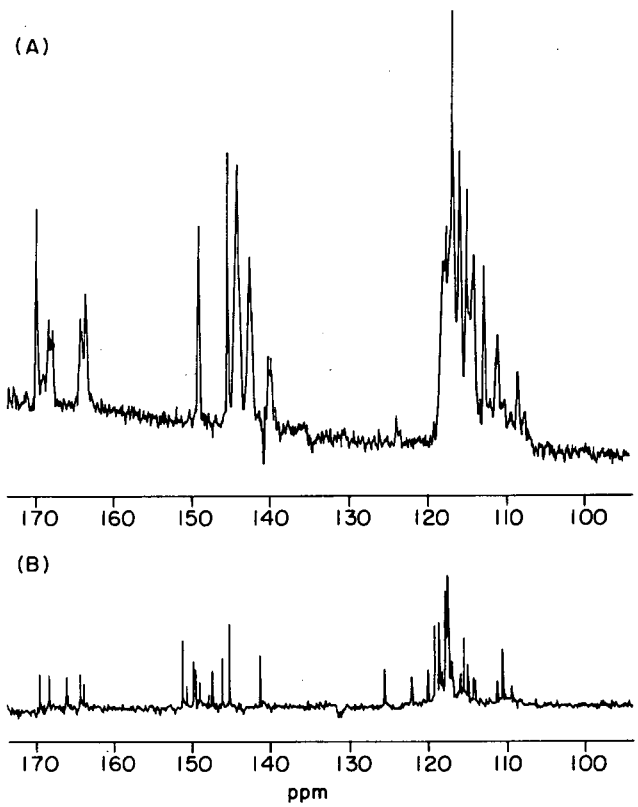

Figure 1. ^{13}C NMR spectrum (100 mz) of (A) arsenic anion (X = H) compound **5** and (B) 3,4-LICAM, **4**, in DMSO-d_6. The region of 100–170 ppm includes the carbonyl region, ~160–170 ppm; aromatic carbon-hydroxyl, ~140–152 ppm; and aromatic carbon, ~110–135 ppm. The methylene carbons, ~0–50 ppm, were masked by the solvent and are not included. (XBL 837-10712)

the ligand, **4** (~140–152 ppm), should show six resonances; however, many more are evident, while the arsenic compound, **5**, has six phenolic carbons appearing at 140 to 150 ppm. The remaining aromatic carbons are in the 110–135 ppm range (12 resonances) for **5**, while the methylene carbons (0–50 ppm, not shown in Fig. 1) were somewhat masked by the solvent, dimethylsulfoxide-d_6.

The UV spectra of **4** and **5** (Fig. 2) indicate that, on formation of the arsenic anion, a pronounced shift from 314 nm (ϵ = 6,576) for **4** to 304 nm (ϵ = 9,001) for **5** (X = H) occurs. A similar occurrence was observed by Raymond *et al.*[7,12] in the coordination of ferric ion with a sulfonated 3,4-LICAM, where the extinction coefficient rose and the wavelength decreased upon complexation of all six phenolic oxygens. The FAB mass spectrum (glycerol) of **5** (X = H) shows a small parent ion at *m/e* 623 (2.5%) and ions at 625 (M+2, 5%) and 626 (M+3, 16%).

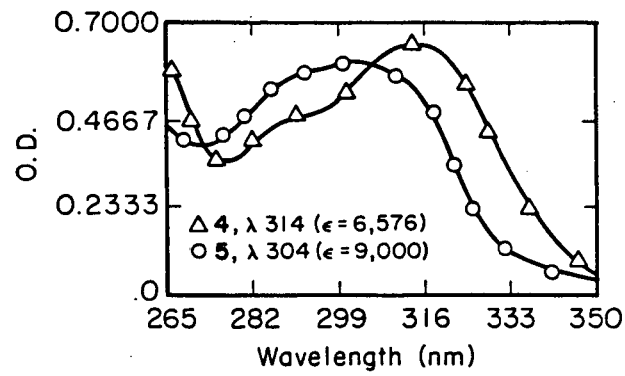

Figure 2. Ultraviolet spectrum of compounds **4** (Δ) and **5** (O) in DMSO. (XBL 837-10710A)

These data support the presumed structure, **5**, including an octahedral configuration around the arsenic; **5** thus represents the first isolated encapsulated arsenic anion structure yet reported. The only other synthesis of a catechol-arsenic anion compound was for catechol itself,[15] and a single-crystal x-ray study provided unequivocal evidence for the distorted octahedral symmetry around arsenic.[16] Although we were unable to prepare a suitable crystalline derivative for x-ray analysis of **5**, a Drieding model indicates that the triscatecholate coordination of **4** around arsenic can readily occur.

PLANNED ACTIVITIES FOR FY 1984

In recent experiments, we have placed **4**, and catechol itself, on a polymer support (10% cross-linked chloromethylated polystyrene-divinylbenzene) and have been able to quantitatively remove arsenate, **1**, from an aqueous ethanol solution, thus verifying the usefulness of this approach in possible synthetic fuel applications.[17,18]

ACKNOWLEDGMENT

We would like to thank Dr. Dexter Sutterfield, Project Manager, Bartlesville Energy Technology Center, for his support.

REFERENCES

1. Brinckman, F.E., and Fish, R.H., Eds. (1981), *Environmental Speciation of Trace Metal-Containing Compounds in Energy-Related Processes*, National Bureau of Standards Special Publication.
2. Fish, R.H., Tannous, R.S., Weiss, C.S., and Brinckman, F.E. (1983), *J. Chem. Soc. Chem. Commun.*, Issue No. 9, p. 490.

3. Brinckman, F.E., Weiss, C.S., and Fish, R.H. (1983), in *Chemical and Geochemical Aspects of Fossil Energy Extraction,* Chap. 13, T.F. Yen, F.K. Kawahara, and R. Hertzberg, Eds., Ann Arbor Science Publishers Inc., Ann Arbor, MI.
4. Fish, R.H., Brinckman, F.E., and Jewett, K.L. (1982), *Environ. Sci. Technol. 16,* p. 174.
5. Fish, R.H., and Tannous R.S. (1982), *Organometallics 1*, p. 1238.
6. Weitl, F.L., Raymond, K.N., Smith, W.L., and Howard, T.R. (1978), *J. Am. Chem. Soc. 100*, p. 1170.
7. Weitl, F.L., Harris, W.R., and Raymond, K.N. (1979), *J. Med. Chem. 22*, p. 1281.
8. Carrano, C.J., and Raymond, K.N. (1979), *J. Am. Chem. Soc. 101*, p. 5401.
9. Harris, W.R., and Raymond, K.N. (1979), *J. Am. Chem. Soc. 101*, p. 6534.
10. Harris, W.R., *et al.* (1979), *J. Am. Chem. Soc. 101*, p. 6097.
11. Weitl, F.L., and Raymond, K.N. (1980), *J. Am. Chem. Soc. 102*, p. 2289.
12. Harris, W.R., Raymond, K.N., and Weitl, F.L. (1981), *J. Am. Chem. Soc. 103*, p. 2667.
13. Pecoraro, V.L., Wong, G.B., and Raymond, K.N. (1982), *Inorg. Chem. 21*, p. 2209.
14. Kappel, M.J., and Raymond, K.N. (1982), *Inorg. Chem. 21*, p. 3437.
15. Ryschkewitsch, G.E., and Garrett, J.M. (1968), *J. Am. Chem. Soc. 90*, p. 7234.
16. Kobayashi, A., Ito, T., Marumo, F., and Saito, Y. (1972), *Acta. Cryst. B28*, p. 3446.
17. Fish, R.H., and Tannous, R.S. (in preparation).
18. Fish, R.H., and Tannous, R.S. (1983), submitted to *Inorg. Chem.*; LBL-16810.

Molecular Characterization of Vanadyl and Nickel Porphyrin and Nonporphyrin Compounds in Heavy Crude Petroleums and Their Asphaltenes*†

R.H. Fish, J.J. Komlenic, and B.K. Wines

The occurrence of vanadyl and nickel nonporphyrin compounds in heavy crude petroleums has been speculated for many years.[1,2] Despite numerous studies attempting to identify vanadyl or nickel nonporphyrin compounds,[3] not a single molecular structure has yet been confirmed. Most of these studies have been limited the lack of a suitable detector. Metallo-nonporphyrin compounds, unlike metallo-porphyrins, have no readily discernible ultraviolet-visible spectra, and the large number of possible vanadyl and nickel compounds in petroleums causes severe separation problems.

Recently, however, the use of on-line, element-selective graphite-furnace atomic-absorption detection for high-performance liquid chromatography systems (HPLC-GFAA) has proved highly effective for the molecular characterization of trace-metal compounds in complex matrices such as shale oil, oil-shale retort waters[4–7] and heavy crude petroleums.

We have described elsewhere[7] the use of an automatically coupled HPLC-GFAA combination to categorize, according to molecular weight and polarity, the vanadyl nonporphyrin and porphyrin compounds in heavy crude petroleums. This technique enabled us to profile or fingerprint vanadyl compounds present in four petroleums and their extracts, and to estimate their molecular-weight distribution. Additionally, the molecular characterization of these compounds was attempted by comparing the GFAA histogrammic retention behavior of vanadium and rapid-scan UV-visible absorbance spectra of HPLC-separated petroleum samples to that of known model vanadyl porphyrin and nonporphyrin standards.

We can now report reverse-phase (C-18 column) HPLC-GFAA analysis of the vanadyl and nickel compounds extracted, using pyridine as solvent, from the same four heavy crude petroleums analyzed earlier; namely, Boscan, Cerro Negro, Wilmington, and Prudhoe Bay. Although reverse-phase separations of demetallated ligands have been discussed before, the use of similar separation techniques with element-selective detection of metal-containing petroleum samples has not previously been reported. We also present HPLC-GFAA vanadium profiles using size-exclusion chromatography (SEC) for the n-pentane–precipitated asphaltenes, maltenes, and asphaltene extracts of the four petroleums. Asphal-

*This work was supported by the Assistant Secretary for Fossil Energy and the Division of Oil, Gas, and Shale Technology of the U.S. Department of Energy through the Bartlesville Energy Technology Center under Contract No. DE-AC03-76SF00098.

†We wish to dedicate this report to Dr. Ted Vermeulen, our colleague, who passed away October 28, 1983.

tenes, the hydrocarbon-insoluble fraction of petroleum, are an extremely abundant source of trace-metal compounds. However, asphaltenes also contain the majority of the high-molecular-weight, aromatic compounds and heteroatoms present in petroleums, which has made the structural characterization of vanadyl nonporphyrin compounds in asphaltenes difficult to accomplish. Finally, we compare the rapid-scan UV-vis profiles, using reverse-phase separations, of the four petroleums and their asphaltene pyridine extracts.

The point of this study is that vanadyl and nickel nonporphyrin compounds—which are thought to account for approximately 50 to 80% of the metals present—must be characterized molecularly in order to design innovative methods of trace-metal removal.[5] In addition, knowing the molecular environment associated with both vanadium and nickel in heavy crude petroleums and asphaltenes will also improve understanding of the biogeochemical mechanisms responsible for the inclusion of these metals in the diagenesis and maturation process of petroleum formation.

ACCOMPLISHMENTS DURING FY 1983

Analysis of Petroleum Extracts

Reverse-Phase HPLC-GFAA Data

Since our previously obtained HPLC-GFAA profiles of SEC-separated crude petroleum extracts had indicated the presence of low-molecular-weight vanadyl compounds (<400 daltons),[7] we were interested in obtaining the reverse-phase HPLC-GFAA vanadium and nickel histogrammic distributions of pyridine extracts from the four petroleums, using various vanadyl and nickel standards (Fig. 1) to verify retention times.

Figure 2 shows the HPLC-GFAA data, obtained using ODS (C18) column, for the standards and the Boscan and Cerro Negro crude petroleum extracts. Each chromatogram consists of a conventional UV-vis absorbance trace (wavelength monitored as designated) and corresponding nickel (232 nm) and vanadium (318.4 nm) histogrammic profiles.

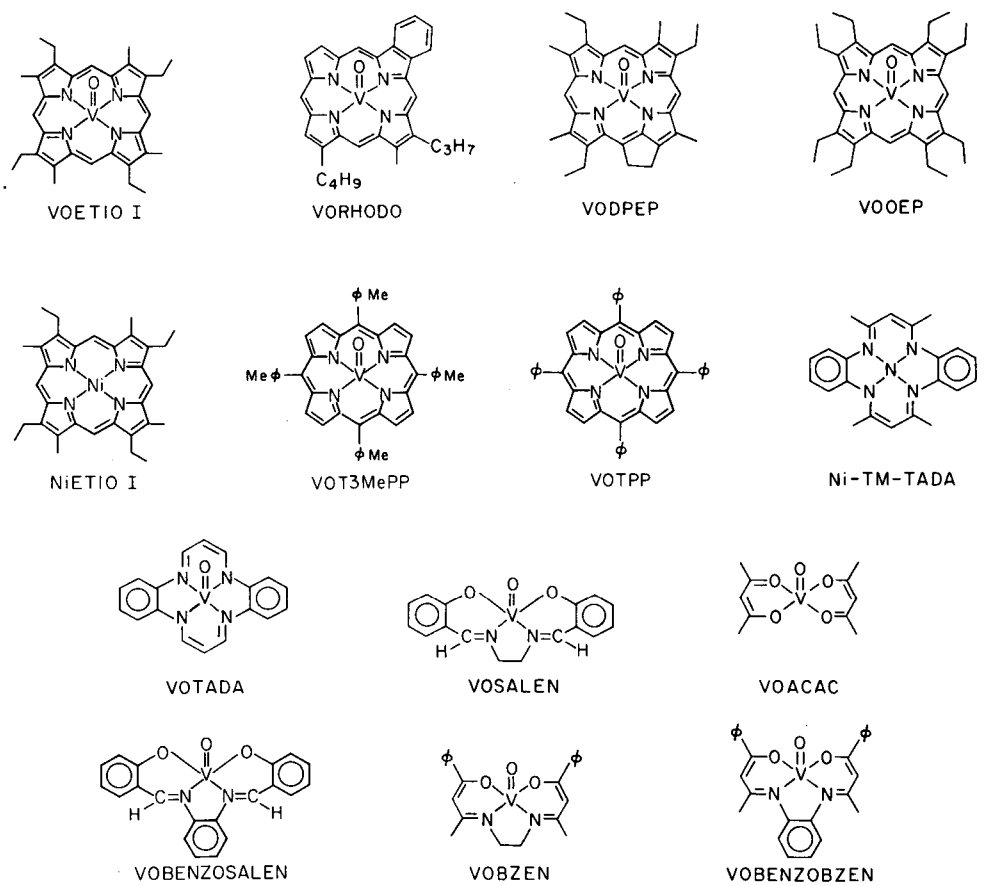

Figure 1. Model nickel and vanadyl porphyrin and nonporphyrin compounds. (XBL 8211-3357A)

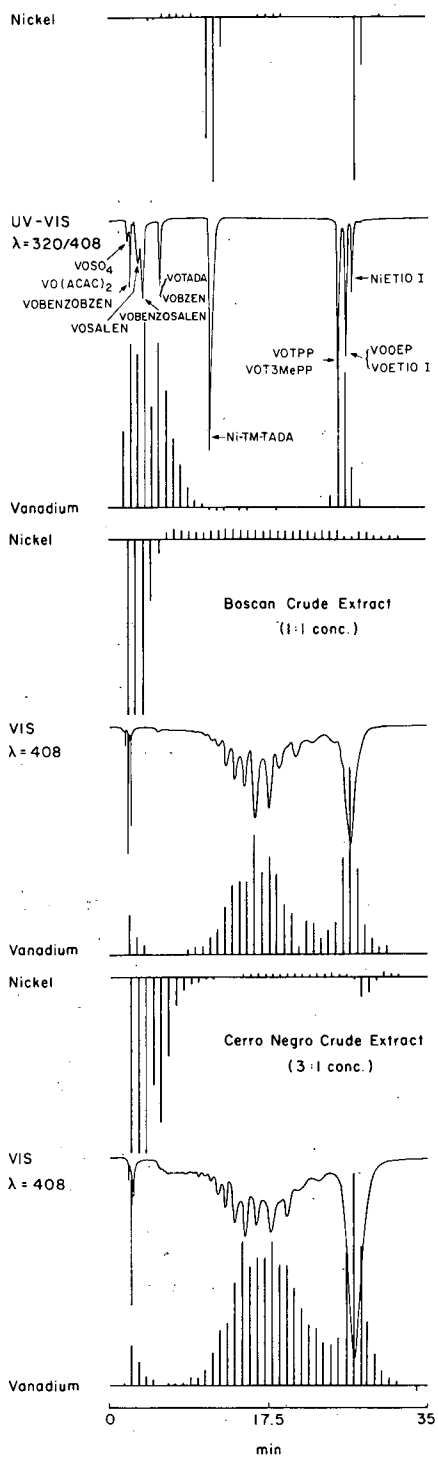

Figure 2. Coupled high-performance liquid chromatography–graphite-furnace atomic absorption data for nickel and vanadyl standards (top) and for Boscan and Cerro Negro crude-oil extracts. (XBL 833–8724)

The model vanadium and nickel nonporphyrin standards (monitored at 320 nm) elute before the porphyrin standards (monitored at 408 nm), indicating the highly polar nature of the former compounds. The nickel compounds extracted from crude petroleums appear to be highly polar and definitely have non-porphyrin ligands. In contrast, the vanadium compounds elute at moderate to low polarities, as determined by the retention behavior of the standards; they thus contain predominantly vanadyl porphyrins in the second band (~17.5 min), while the third band contains both porphyrin and nonporphyrin compounds.

Figure 3 shows similar ODS-HPLC-GFAA data for Wilmington and Prudhoe Bay petroleum extracts. These extracts also show that most of the extracted nickel compounds associated with the highly polar nickel standards; however, Wilmington extract also contains a sizable fraction of low-polarity (possibly porphyrinic) nickel compounds. Both extracts also show moderate to low polarity for most of the vanadyl compounds.

Although reverse-phase separations of petroleum samples have been studied,[3] we do not believe that the occurrence of these highly polar nickel compounds have been verified before. Figure 3 also indicates that reverse-phase separations of the pyridine extracts give better resolution than normal-phase analysis.[8,9] In fact, these separations rival those reported for demetallated complexes,[10] thus calling into question the usefulness of current demetallation procedures for the analysis of petroleum extracts.

Rapid-Scan Data

Unfortunately, we could not scan the highly polar, ODS-separated nickel peaks because of their sharpness; the maximum scan rate of 20 nm/sec sets a limit on the peak width that can be scanned. The highly polar nickel fractions were therefore collected and their UV-vis spectra obtained off-line, using a Cary 219 spectrophotometer. Maximum absorbances (above background) for these fractions were observed between 280 and 300 nm. The lack of any observable Soret absorbance strongly suggests a predominance of nickel nonporphyrin compounds.

It is not surprising that these nickel nonporphyrin fractions have not previously been found because most attempts to identify metallo-porphyrins in crude petroleums have used column chromatography on silica or alumina packing to isolate the porphyrins.[3] The highly polar nickel compounds shown in Fig. 3 are probably irreversibly bound to the column packing during elution. Although solvent-selective extraction has not been used much in recent research, the technique prevents the loss of nickel nonporphyrins through interaction with a fractionat-

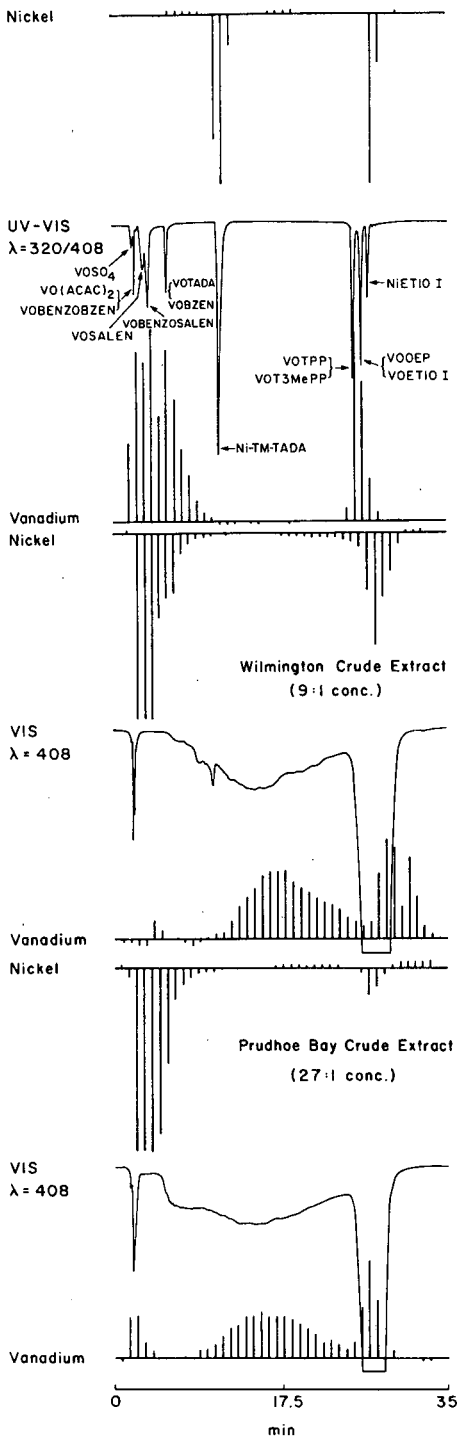

Figure 3. HPLC-GFAA data for Wilmington and Prudhoe Bay crude-oil extracts, compared with nickel and vanadyl standards (top). (XBL 833–8738)

ing column. The use of reverse-phase HPLC also prevents the loss of extractable polar compounds that could be irreversibly retained on a normal-phase column.[2]

This discovery—that most of the extracted nickel exists as highly polar nonporphyrin compounds, in contrast to vanadium, which is associated primarily with moderate- and low-polarity compounds—has important implications for catalyst deactivation.[11] Currently, most catalyst deactivation modeling studies use vanadyl and nickel porphyrins exclusively. However, since porphyrins are known to account only in part for the two metals, the relevancy of these studies must be reexamined, especially with regard to the reactivity of acid-unstable metallo-nonporphyrin ligands.[1]

Scan data for the ODS-separated moderate- and low-polarity vanadium-containing bands for Boscan and Cerro Negro extract have been obtained. Rapid-scan data for Boscan extract at 16 minutes shows a "relatively clean" vanadyl porphyrin spectrum. However, the other three spectra show varying UV background absorbances at less than 400 nm, indicating the presence of distinctly nonporphyrinic species in these fractions. Similar rapid-scan data obtained for Wilmington and Prudhoe Bay extracts have also been obtained. The absence of discernible Soret absorbance strongly suggests the presence of vanadyl nonporphyrin compounds as major vanadium constituents in Prudhoe Bay and Wilmington crude petroleum extracts.

Unfortunately, we have been unable so far to obtain model vanadyl nonporphyrin compounds of moderate to low polarity. Nevertheless, the identification of fractions in these extracts that are rich in vanadium and nickel nonporphyrins is very important. These fractions are currently being submitted to off-line analysis via high-resolution mass spectroscopy, electron-spin resonance, and other techniques to accurately ascertain the molecular environment associated with the metal. It will be interesting from a biogeochemical perspective to determine if these compounds are porphyrin derivatives, i.e., hydrogenated porphyrins, or uniquely nonporphyrinic species, possibly incorporating sulfur into the ligand ring structure.

Analysis of the n-Pentane–Precipitated Asphaltenes

Analyses of the results of the 40:1 n-pentane precipitation have been conducted. Approximately 49% to 77% of the vanadium is precipitated as asphaltenes, even though this fraction constitutes only 4% to 23% by weight of the petroleum. Similarly, a large fraction of nickel is also precipitated as asphaltenes at concentrations constituting ~39% to 78% of the nickel present.

The results of the extraction of the precipitated asphaltenes reveal that only 5% to 18% by weight of the vanadium present has been extracted. This behavior is very different from that observed for the extraction of the crude petroleums,[7] from which upwards of 50% of the vanadium was removed. Previously, we had observed that a considerable percentage of vanadyl nonporphyrin compounds could be removed from the high-molecular-weight asphaltenic component of heavy crude petroleums by using solvent-selective extraction techniques.[12] A significantly lower percentage of vanadyl compounds is extracted from the n-petane–precipitated asphaltenes; this finding has importance for the use of asphaltenes as starting materials for the identification of vanadyl porphyrin and nonporphyrin compounds in heavy petroleums.

SEC-HPLC-GFAA Analysis

Clearly, a better understanding of the types and distribution of vanadyl and nickel compounds present in n-pentane asphaltenes was needed. We decided to analyze the n-pentane–precipitated asphaltenes, the maltenes, and the pyridine extracts of each petroleum, using the SEC-HPLC-GFAA technique. These separations for Prudhoe Bay and Wilmington were obtained using a 50/100/1000 Å SEC column combination (Figs. 4 and 5). The visible absorbance was monitored at 408 nm, corresponding to the Soret band of vanadyl porphyrins identified in crude oils,[13] and the GFAA detector was set at 318.4 nm, specific for vanadium.

Calibration for the low-molecular-weight regions was accomplished using the standards from Fig. 1. In comparison to the more traditional use of polystyrenes,[3] use of vanadyl compounds as calibration standards should increase the accuracy of molecular weight determinations for vanadyl compounds present in petroleum. Polystyrene standards have, however, been used to calibrate the high molecular weights (>900 daltons), since no vanadyl compounds at these molecular weights were available.

Because of the interactions that may occur between the complex petroleum matrix and the SEC column,[14] our molecular weight categories are for comparison purposes and are not regarded as absolute. Boscan asphaltene registers continuous visible absorbance and yields vanadium profiles over the entire molecular weight region. The maximum absorbance for the visible spectrum and for vanadium detection occurs in the lowest molecular weight range, i.e., to less than 400 daltons, with very little vanadium present at molecular weights greater than 10,000 daltons. As expected from the structural

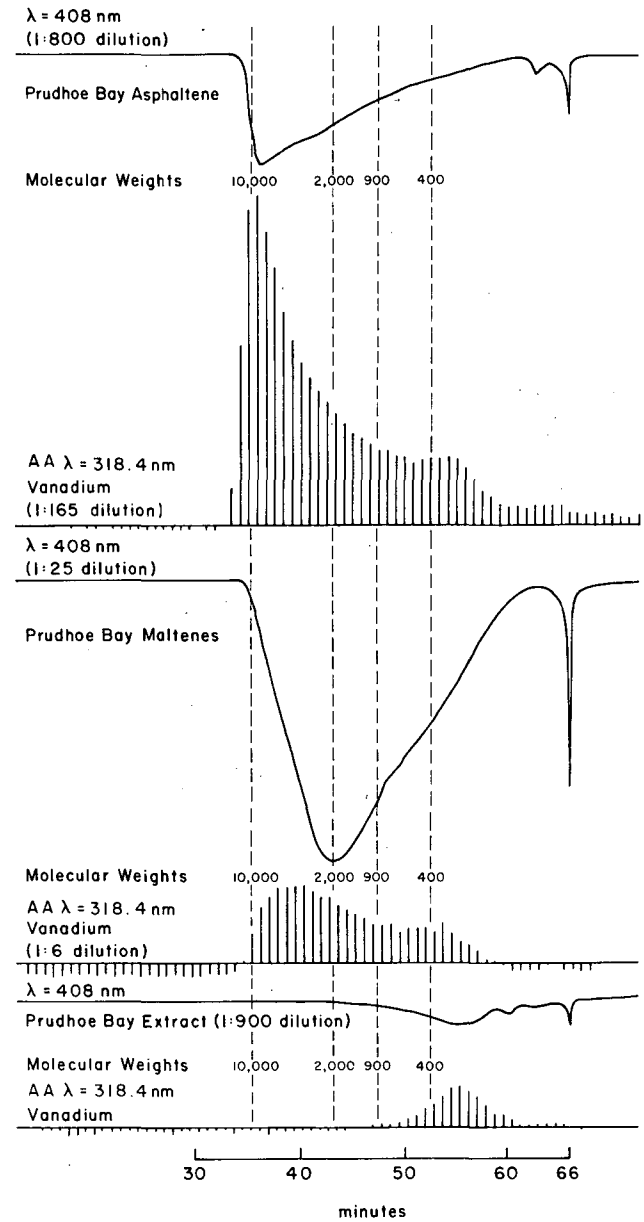

Figure 4. Molecular-weight distribution profiles of Prudhoe Bay asphaltene, maltene, and pyridine extracts, from 50/100/1000 Å size-exclusion chromatography column combination. (XBL 8210–3113)

differences between the maltene and asphaltene fractions,[15] the maltene vanadium absorbances are skewed toward lower average molecular weights than are the corresponding asphaltenes. Most notable is the deficiency of vanadium compounds in the range above 2,000 daltons compared to the asphaltene profiles. The pyridine extract of Boscan asphaltene has a vanadium maximum corresponding to 380 daltons, which is too low to represent porphyrins with alkyl substituents. Thus, most of the compounds present

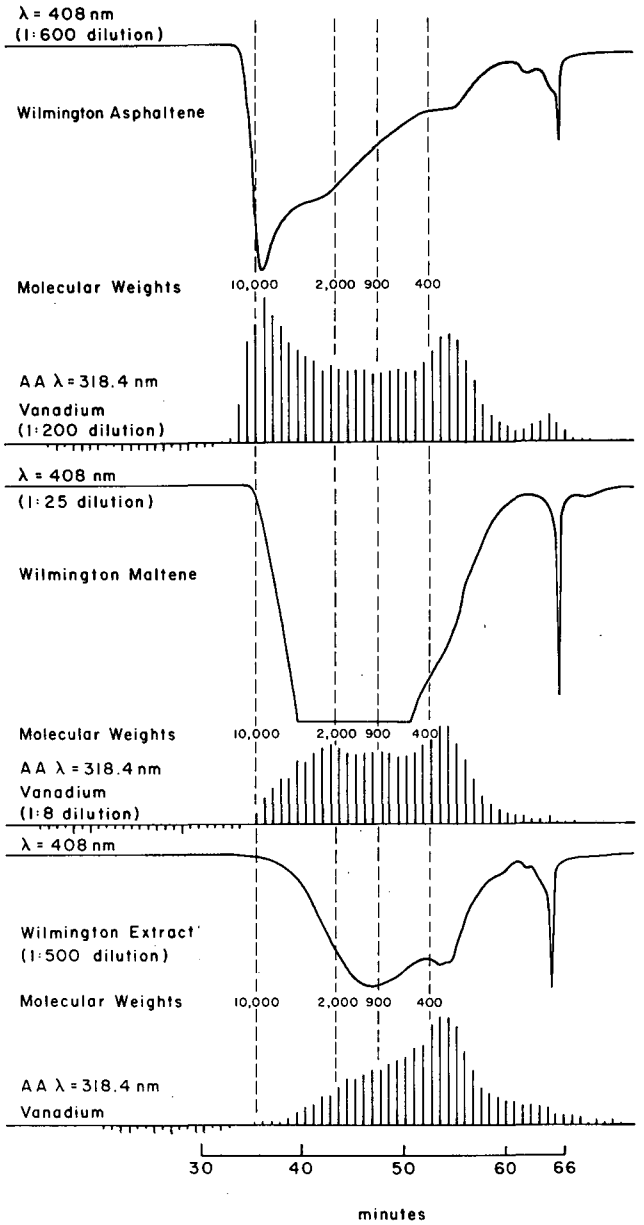

Figure 5. Molecular-weight distribution profiles of Wilmington asphaltene, maltene, and pyridine extracts, from same SEC-column combination as for Prudhoe Bay Oil (Fig. 4). (XBL 8210–3114)

in the extracts must be considered nonporphyrinic, on the basis of the SEC calibration data for the standards in Fig. 1.

Similar data for Prudhoe Bay asphaltene were also obtained (Fig. 4). A significantly greater percentage of vanadium associated with Prudhoe Bay asphaltene is present above 2000 daltons compared to Boscan asphaltene. However, Prudhoe Bay maltene, like Boscan maltene, shows a trend toward lower average molecular weights and also registers a predominance of extractable low-molecular-weight (<400 daltons) vanadyl compounds.

The quantitative distribution of vanadyl compounds by molecular weight used a calibration curve previously reported by Fish and Komlenic.[7] The vanadyl compounds were divided into five categories of molecular weight: greater than 9,000 daltons; 9,000–2,000 daltons; 2,000–900 daltons; 900–400 daltons; and less than 400 daltons. The percent vanadium was then determined by summing the peak heights, which had been automatically digitized using an integrator.

The results show Wilmington and Prudhoe Bay asphaltenes as having greater percentages of vanadium in the very high-molecular-weight region (>2,000 daltons) than do the asphaltenes of the two Venezuelan petroleums. Furthermore, the Boscan, Cerro Negro, and Prudhoe Bay maltenes show proportionately less vanadium below 400 daltons than do the whole petroleums. Wilmington maltene, in contrast, has proportionately less vanadium above 2000 daltons and has more vanadium in the porphyrinic molecular weight region than the petroleum itself.

Interestingly, vanadyl compounds extracted from the asphaltenes of all four petroleums are predominantly at the low molecular weights (<400 daltons), indicating vanadyl nonporphyrin compounds. Previously, we had found that vanadyl compounds (molecular weight < 900 daltons) are contained in extracts of each heavy crude petroleum. We also confirmed that these low-molecular-weight vanadyl complexes can be extracted from the n–pentane–precipitated asphaltenes of each petroleum as well. Although each asphaltene shows that most of the extractable vanadyl compounds have molecular weights of less than 400 daltons, only 5–18 wt% of the vanadium was extracted, as compared to 50–87 wt% for heavy crudes.[6] Thus, vanadyl compounds of similar molecular weight are extracted from both petroleum and asphaltene sources. However, significant differences must exist between vanadyl complexes extracted from the whole petroleums and the n-pentane–precipitated asphaltenes.

Reverse-Phase HPLC-GFAA

Figure 6 compares the ODS-HPLC-GFAA data for the standards and the Boscan asphaltene extract monitored at both 320 and 408 nm. Like the Boscan whole-crude petroleum extract, the majority of the nickel compounds elute with the highly polar standards, while the vanadyl compounds are primarily associated with low to moderate polarities. ODS-

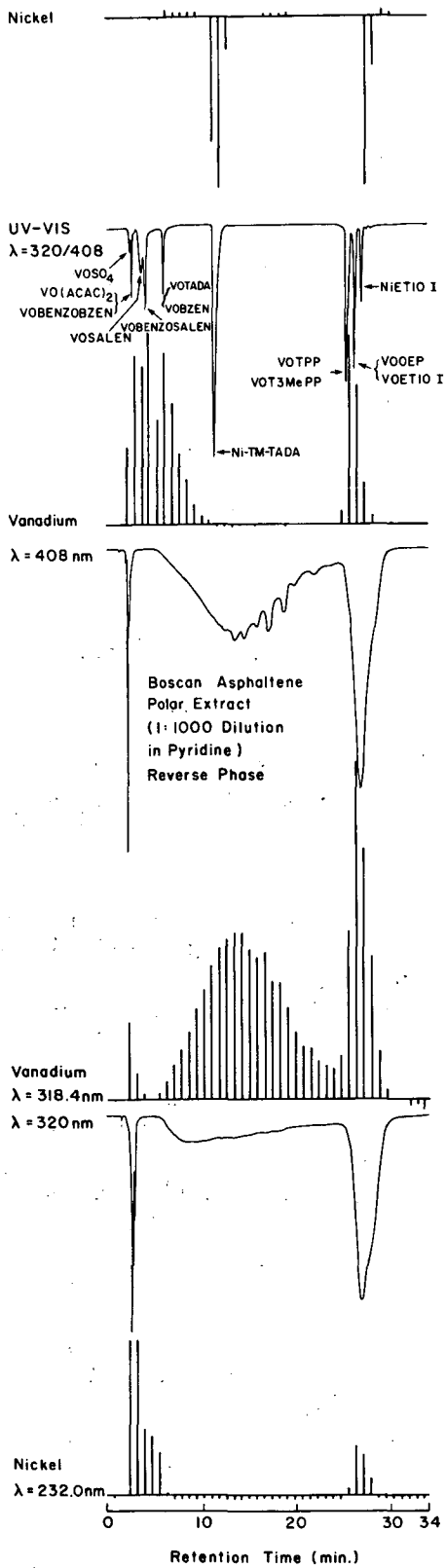

Figure 6. Comparison of ODS-HPLC-GFAA retention times for the molecular standards (top) and for Boscán whole crude at both 408 nm (middle) and 320 nm (bottom). Profiles for the other oils are similar.

(XBL 833–8787)

HPLC-GFAA analyses of Cerro Negro, Wilmington, and Prudhoe Bay asphaltene extracts show similar metal profiles to those for the petroleum extracts, so they are not reproduced here. Wilmington asphaltene extract, however, does show a fraction of nonpolar nickel eluting, indicating that some nickel porphyrin compounds have also been extracted.

Rapid-Scan Data

Rapid-scan data have been studied (Fig. 7). In comparison to the rapid-scan UV-vis spectra of the whole crude petroleum extracts, the four asphaltene extracts generally show greater Soret absorbances, indicating increased concentrations of vanadyl porphyrin compounds being extracted.

Comparison of the Petroleum and Asphaltene Results

The extraction of the precipitated asphaltenes removed only 5% to 18% of the vanadium, compared to the removal of 50% to 87% of the vanadium in the whole petroleums.[7] Larger micelles in the precipitated asphaltenes could account for this difference, since asphaltenes are by definition a solubility class, and the choice of precipitating solvent is known to have a noticeable effect on the mass and aromaticity of precipitated asphaltenes.[16] Further, vapor-pressure osmometry studies of asphaltene molecular weights have demonstrated that the degree of association between asphaltene molecules is strongly influenced by the polarity and functionality of the solvent used in the measurements.[17]

An equilibrium apparently exists between the interactions of asphaltene molecules with each other and with the solvent. In two whole petroleums, the resins form a very complex solvent in which the asphaltenes are dispersed. When asphaltenes are precipitated, the asphaltene-resin interactions become weakened and the asphaltene-asphaltene interactions dominate, forming larger micelles. Nonpolar solvents such as p-xylene are ineffective in breaking up the large micelles in precipitated asphaltenes, and many vanadyl compounds, entrapped during the precipitation, are inaccessible to extraction.

Methylene chloride is a much more effective solvent for breaking up asphaltene micelles than xylene. This can be seen by comparing the 50/100/1000 Å SEC-HPLC-GFAA analysis of the heavy crude petroleums[7] with the similar analysis of the asphaltenes and maltenes reported here.[18] Methylene chloride was used as the injection solvent for all these analyses, and a mass balance of the vanadium present in each molecular-weight region shows that

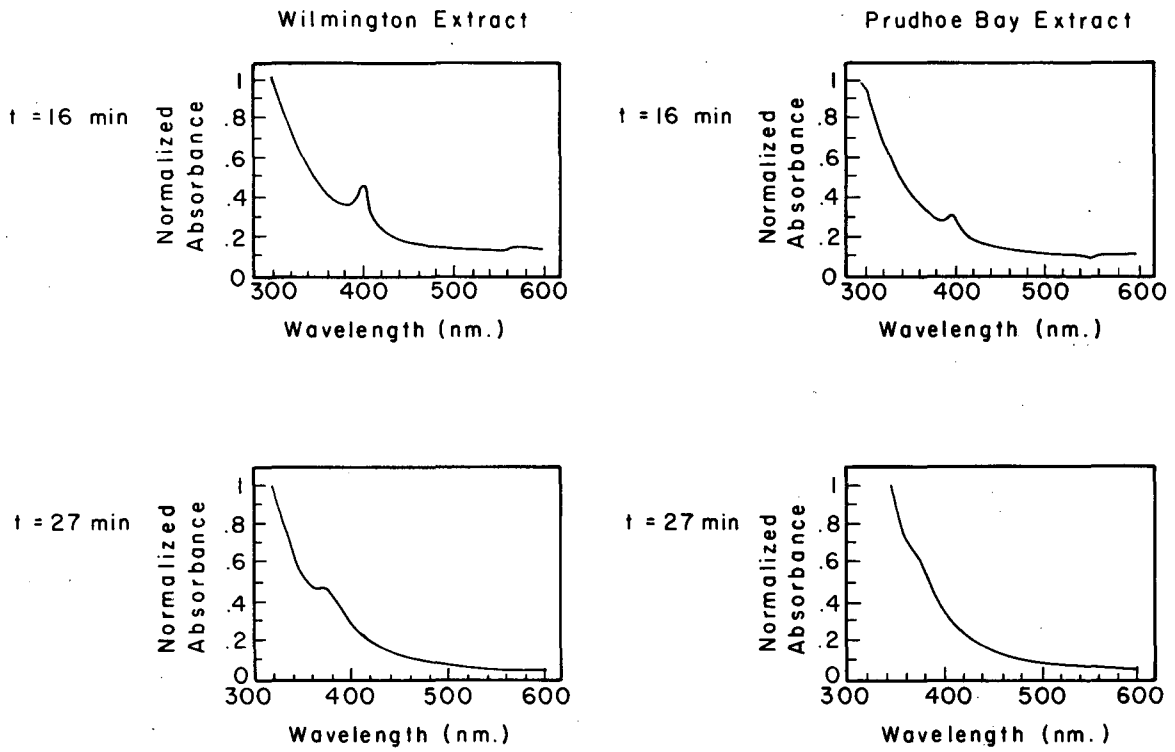

Figure 7. Reverse-phase HPLC rapid-scan analysis of UV-visible spectra of polar extracts from asphaltenes: left, Wilmington extract; right, Prudhoe Bay extract. Time for upper profiles, 16 min; lower profiles, 27 min. (XBL 833-8739)

the vanadium in the maltenes and asphaltenes of a given region add up to the vanadium present in the same region of the whole crude petroleum. Clearly, methylene chloride is sufficiently polar to overcome intermicellular forces in the crude petroleum as well as in the precipitated asphaltenes.

SEC-HPLC-GFAA analysis of the extracted asphaltenes failed to show a reduction in the amount of vanadium present at molecular weights over 2000 daltons. This suggests that some mechanism reentraps the low-molecular-weight vanadyl compounds into the high-molecular-weight asphaltenic fraction of the petroleum. The extracts have almost no vanadyl compounds at molecular weights over 900 daltons. Rapid-scan analysis of the reverse-phase HPLC-GFAA–separated asphaltene pyridine extracts has shown the concentration of vanadyl porphyrins to be higher in the asphaltene extracts than in the extracts of whole crude petroleums. Despite studies indicating that asphaltenes have higher concentrations of vanadyl nonporphyrins than maltenes,[19] the relative abundance of vanadyl porphyrins versus vanadyl nonporphyrins in precipitated asphaltenes needs to be reevaluated. Our work indicates that the precipitation of asphaltenes accomplishes a desired separation by selectively precipitating vanadyl porphyrins; the maltenes should thus be excellent sources of vanadyl nonporphyrin compounds.[20]

Because nickel is generally present in crude petroleums at lower concentrations than vanadium, relatively little research has been directed at identifying nickel compounds.[3] In experiments in which column chromatography has been used to remove vanadyl porphyrins from the petroleum matrix, a light pink band eluting before the bright red vanadyl porphyrin band has generally been assumed to contain nickel porphyrins, but little work has actually been done to identify the constituents of this band.

The results of the reverse-phase HPLC-GFAA analysis show that very little of the nickel in the petroleum asphaltene extracts is actually present as nickel porphyrins. In Boscan, Cerro Negro, and Prudhoe Bay extracts, over 90% of the nickel is nonporphyrin. Wilmington is the exception, with a third of the nickel eluting at a retention time consistent with nickel porphyrins. This high concentration of nickel porphyrins in the Wilmington extracts could be a consequence of less severe aging than in the other three petroleums. Nickel, because of its smaller size and greater symmetry, coordinates more readily with the porphyrin ring than does vanadyl ion.[21] However, during maturation of the

petroleum, the nickel could be replaced by vanadyl ion, which forms more stable metallo-porphyrin complexes.[22] Wilmington is not the youngest or the least buried petroleum of the four studied, but it does have the least severe combination of these two factors.

This discovery of large amounts of nickel nonporphyrins has a direct bearing on current research in refinery catalyst poisoning by trace metals. Since it has been generally accepted that a substantial fraction of the nickel in heavy crude petroleums is coordinated in porphyrin rings, studies of the poisoning mechanisms have used nickel porphyrins to model the naturally occurring nickel compounds.[11] As most of the suspected nonporphyrin chelating systems are less stable with respect to demetallation than porphyrins, these studies fail to adequately model the deposition of nickel nonporphyrins on catalysts. Before modeling studies of nickel poisoning can be improved, it will be necessary to isolate and identify these nickel nonporphyrins.

Such identification should also provide important biogeochemical information. Knowing the structures of these compounds should give insight into their sources in the petroleum feedstock. Reverse-phase analyses demonstrated that most of the extracted vanadyl nonporphyrins were not comparable to the model vanadyl nonporphyrins available. Both normal and reverse-phase analyses demonstrate that a significant fraction of the eluting compounds with vanadyl nonporphyrin spectra did not correspond with the elution times of the model vanadyl nonporphyrins.

In future work, it will be necessary to have a greater array of model metallo-nonporphyrin compounds. Among the compounds that should be considered are the hydrogenated vanadyl porphyrins. In the reducing environment of the crude petroleum reservoir,[23] it is possible that the porphyrin rings may become hydrogenated, and there has been a report of nonmetallated, hydrogenated porphyrins in shale.[24–26] If the ring is sufficiently hydrogenated, the stability of the metallo-porphyrin may be weakened to the point where demetallation and decomposition of the porphyrin ring become possible. This may represent a mechanism by which porphyrins have been demetalled in older petroleum deposits.

PLANNED ACTIVITIES FOR FY 1984

We plan to continue our studies on the characterization of vanadyl and nickel compounds, using high-resolution mass spectrometry and electron spin resonance techniques.

REFERENCES

1. Yen, T.F. (1975), in *The Role of Trace Metals in Petroleum*, Chaps. 1 and 10, T.F. Yen, Ed., Ann Arbor Science, Ann Arbor, MI.
2. Dickson, F.E., Junesh, C.J., Mcginnis, E.L., and Petrakis, L. (1972), *Anal. Chem. 44*, p. 978.
3. Spencer, W.A., Galobardes, J.F., Curtis, M.A., and Rogers, L.B. (1982), *Sep. Sci. and Technol. 17*, p. 797.
4. Fish, R.H., Brinckman, F.E., and Jewett, K.L. (1982), *Environ. Sci. Technol. 16*, p. 174.
5. Fish, R.H. and Tannous, R.S. (1982), *Organometallics 1*, p. 1238.
6. Fish, R.H., Tannous, R.S., Walker, W.S., Weiss, C.S., and Brinckman, F.E. (1983), *J. Chem. Soc. Chem. Commun. 2*, p. 490.
7. Fish, R.H. and Komlenic, J.J. (1984), *Anal. Chem.*, in press.
8. Weiss, C.S., Jewett, K.L., Brinckman, F.E., and Fish, R.H. (1981), *Environmental Speciation and Monitoring Needs for Trace Metal-Containing Substances from Energy-Related Processes,* F.E. Brinckman and R.H. Fish, Eds., National Bureau of Standards Special Publication 618, Washington, D.C.
9. Barwise, A.J.G. and Whitehead, E.V. (1979), *Phys. Chem. Earth 12, p. 181.*
10. Eglinton, G., Hajibrahim, S.K., Maxwell, J.R., and Quirke, J.-M.E. (1979), *Anal. Chem. 12*, p. 193.
11. Hajibrahim, S.F. (1981), *Liq. Chrom. 4*, p. 749.
12. Hung, C.W. and Wei, T. (1980), *Ind. Eng. Chem. Process Des. Dev. 19*, pp. 227 and 250.
13. Agrawal, R. (1980), Ph.D. dissertation, Massachusetts Institute of Technology.
14. Baker, E.W. (1969), *Organic Geochemistry*, G. Eglinton and M.T.J. Murphy, Eds., Springer-Verlag, Berlin.
15. Sugihara, J.M., Branthaver, J.F., Wu, G.Y., and Weatherbee, C. (1970), *Am. Chem. Soc., Div. Petrol. Chem., Preprints 15,* p. C5.
16. Friley, B.K., Phelps, J.B., and Kincaid, J.R. (1983), *J. Chrom. 258*, p. 310.
17. Filby, R.H. (1975), in *The Role of Trace Metals in Petroleum*, Chap. 2, T.F. Yen, Ed., Ann Arbor Science, Ann Arbor, MI.
18. Long, R.B. (1979), *Am. Chem. Soc., Div. Petrol. Chem., Preprints 24,* p. 891.
19. Moschopedis, S.P., Fryer, J.F., and Speight, J.G. (1976), *Fuel 55,* p. 227.
20. Komlenic, J.J., Vermeulen, T., and Fish, R.H. (1982), "Molecular Characterization and Fingerprinting of Vanadyl Porphyrin and Non-Porphyrin Compounds in Heavy Crude

Petroleums Using HPLC-GFAA Analysis," M.S. thesis by J.J. Komlenic, University of California, Berkeley, LBL-15397.
21. Erdman, J.G. and Harju, P.H. (1963), *J. Chemical Engineering Data 8(2)*, p. 252.
22. Wines, B.K., Vermeulen, T., and Fish, R.H. (1983), "Molecular Characterization and Fingerprinting of Vanadyl Porphyrin and Non-Porphyrin Compounds in the Asphaltenes of Heavy Crude Petroleums Using HPLC-GFAA Analysis," M.S. thesis by B.K. Wines, University of California, Berkeley, LBL-16867.
23. Sugihara, J.M. and Branthaver, J.F. (1976), *Am. Chem. Soc., Div. Petrol. Chem., Preprints 21*, p. 411.
24. Erdman, J.G., Walter, J.C., and Hanson, W. (1957), *Am. Chem. Soc., Div. Petrol. Chem., Preprints 2(1), p. 259.*
25. Mackenzie, A.S., Brossell, S.C., Eglinton, G., and Maxwell, J.R. (1982), *Science 217*, p. 491.
26. Hodgson, G.W. (1973), *Ann. N.Y. Acad. Sci. 206*, p. 676.

Homogeneous Catalytic Hydrogenation: Selective Reductions of Polynuclear Heteroaromatic Compounds Catalyzed by Chloro-(Tristriphenylphosphine)Rhodium(I)*

R.H. Fish, A.D. Thormodsen, and H. Heinemann†

We recently discovered that the nitrogen heterocyclic ring incorporated in polynuclear heteroaromatic nitrogen compounds can be regioselectively reduced under a variety of homogeneous hydrogenation conditions.[1,2] These results are important because they have practical implications for coal liquefaction and the upgrading of coal liquids and shale oils as well as for the ultimate removal of nitrogen from these synthetic fuels.

In our quest for catalysts that could perform these reductions under rather mild conditions, we discovered that Wilkinson's catalyst—chloro(tristriphenylphosphine)rhodium(I), abbreviated $(\phi_3P)_3RhCl$—can selectively reduce the heterocyclic ring in model polynuclear heteroaromatic nitrogen and sulfur synthetic-fuel compounds.

Although Wilkinson's catalyst is one of the most extensively studied homogeneous hydrogenation catalysts known,[3–6] this is the first time, to our knowledge, that the use of this catalyst for the selective hydrogenation of the model compounds shown in Fig. 1 under homogeneous conditions has been reported.[7] Additionally, we will demonstrate the usefulness of deuterium gas, in place of hydrogen gas, for understanding the mechanisms involved in the reduction of polynuclear heteroaromatic compounds, including reversibility in the hydrogenation of the carbon-nitrogen double bond, i.e., dehydrogenation. There may also be a cyclometallation reaction in the exchange of hydrogen for deuterium in the aromatic ring close to the heterocyclic ring and in the position alpha to the nitrogen atom. We have also attempted to define what potential inhibitory effects other model synthetic fuel constituents would have on the rate of hydrogenation, using quinoline (compound **1**) for these studies.

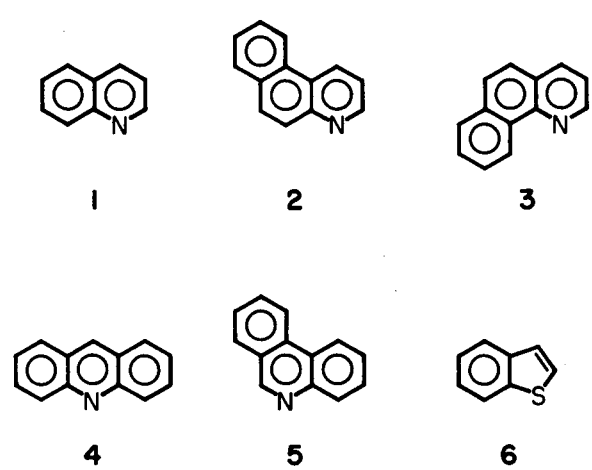

Figure 1. Model synthetic fuel compounds used in hydrogenation reactions with Wilkinson's catalyst: **1**, quinoline; **2**, 5,6-benzoquinoline; **3**, 7,8-benzoquinoline; **4**, acridine; **5**, phenanthridine; and **6**, benzothiophene
(XBL 8211-3297)

*This work was jointly funded by the Director, Office of Energy Research, Office of Basic Energy Sciences, Chemical Sciences Division, and the Assistant Secretary of Fossil Energy, Office of Coal Research, Liquefaction Division of the U.S. Department of Energy through the Pittsburgh Energy Technology Center under Contract No. DE-AC03-76SF00098.

†Materials and Molecular Research Division.

ACCOMPLISHMENTS DURING FY 1983

Selective Hydrogenation

Table 1 contains the relative rate data for the selective reduction of the nitrogen heterocyclic ring (compounds **1–5**) and, in one case, a sulfur heterocyclic ring (compound **6**), catalyzed by $(\phi_3P)_3RhCl$ under a standard set of conditions; Fig. 2 shows the kinetic apparatus used. Turnover numbers ranged from ~35 to ~0.1 per hour at the 10:1 substrate/metal ratio. (The 10:1 ratio was used in all experiments described here.) The order of individual relative rates was **5** >> **4** > **6** > **1** > **2** > **3**, reflecting the contribution of both steric and electronic effects. In only one case (**4**) did we see a change in the selectivity, when a substantial amount of 1,2,3,4-tetrahydroacridine (36%) was formed along with 9,10-dihydroacridine, although at half the rate of the latter product.

Inhibition Studies

To learn about other potential synthetic fuel compounds that might inhibit these hydrogenation reactions, we chose quinoline, **1**, as the model compound. Interestingly, the rate of hydrogenation was not affected by thiophene, **7**, but was totally quenched by pyridine, **8**, and 3-methylpyridine, **9** (1:1 molar ratio of **7**, **8**, and **9** to **1**).[8] Moreover, the rate of hydrogenation of **1** was enhanced by indole, **10**, by a factor of 1.4, while **10** itself was not hydrogenated. In addition, 2-methylpyridine, **11**, slightly retarded the rate as did the product 1,2,3,4-tetrahydroquinoline, **12** (Table 2).

It appears that competitive binding of the substrates to the rhodium metal center is a highly critical parameter that encompasses both steric and electronic effects. For example, **8** (pK_b 8.42) and **12** (pK_b ~9.38) are stronger bases than **1** (pK_b 9.52) with **8** quenching and **12** retarding the rate of hydrogenation of **1**, whereas thiophene, an aromatic sulfur compound, has no effect. While **8** and **9** quench, 2-methylpyridine, **11** (pK_b 8.03), slightly retards the hydrogenation rate of **1**, clearly a consequence of a steric effect in binding at the rhodium metal center.[6,9] At present, we have no definite reason why indole (**10**) enhances the hydrogenation rate of **1**, other than the possibility that it assists in the dissociation of triphenylphosphine from the rhodium metal center to a highly reactive 14-electron species,

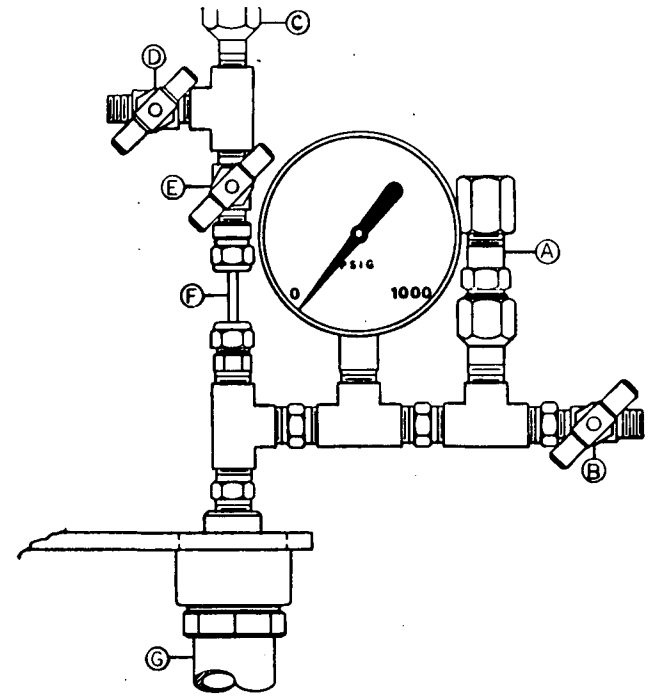

Figure 2. Schematic diagram of the Parr kinetic apparatus for use in hydrogenation rate studies. *A*, rupture disk; *B*, outlet valve; *C*, septum port; *D*, inlet valve; *E*, dip-tube valve; *F*, dip tube; *G*, reactor cup. (XBL 836–10434)

Table 1. Relative rates of reduction of compounds 1–6 under hydrogenation conditions with $(\phi_3P)_3RhCl$ as catalyst.[a]

Substrate[b]	Product[c]	Rate (%/min)[d]	Relative rate[e]
1	1,2,3,4-Tetrahydroquinoline	0.08	1.0
2	1,2,3,4-Tetrahydro-5,6-benzoquinoline	0.03	0.38
3	1,2,3,4-Tetrahydro-7,8-benzoquinoline	0.01	0.13
4	9,10-Dihydroacridine[f]	0.20	2.5
5	9,10-Dihydrophenanthridine	~6	~75
6	2,3-Dihydrobenzothiophene	0.12	1.5

[a]The solvent was benzene and the substrate-to-metal ratio was 10:1. The partial pressure of hydrogen was 310 psi and the temperature was 85°C. See Fig. 2 for schematic of kinetic apparatus.

[b]See Fig. 1.

[c]Analysis by capillary gas chromatography and GC-EIMS.

[d]Pseudo-zero order rate that was followed to ~25% conversion.

[e]The rates are relative to quinoline, which was set to 1.0; i.e., each substrate rate was divided by 0.08%/min to obtain a relative rate.

[f]Another product, 1,2,3,4-tetrahydroacridine (GC-EIMS), was also formed at a rate of 0.12%/min (relative rate 1.5) and represents 36% of total product (64% dihydroacridine).

Table 2. Relative rates of hydrogenation of compound **1** in the presence of other substrates.

Added substrate[a]	H_2 (psi)	Relative rates of hydrogenation of **1**
None	310	1.0
7, Thiophene	310	0.9
8, Pyridine	310	0.0
9, 3-methylpyridine[b]	310	0.05
10, Indole	310	1.4
11, 2-methylpyridine[b]	310	0.6
12, 1,2,3,4-Tetrahydroquinoline	310	0.40

[a]1 m*M* of **1** and 1 m*M* of added substrate and 0.1 m*M* of Wilkinson's catalyst at 77°C (±2°C).
[b]85°C (±2°C).

thus permitting a more facile pathway for quinoline coordination to rhodium.[3–6]

Deuterium Gas Experiments

The substitution of deuterium gas (D_2) for hydrogen gas (H_2) has been shown to be helpful in elucidating the mechanisms and stereochemistry of homogeneous hydrogenation reactions.[5,6] The reaction of **1** with D_2 gas (500 psi) and $(\phi_3P)_3RhCl$ at 80°C for 48 h (10:1 substrate-to-metal ratio), followed by gas chromatography–electron impact mass spectrometry (GC-EIMS) and 400 MHz ^1H nuclear magnetic resonance spectroscopy (NMR), provided the results depicted in Eq. (1).

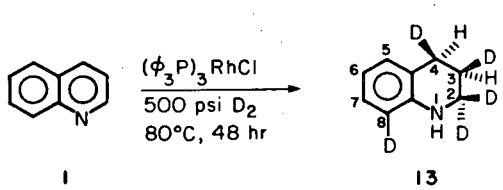

(1)

The reaction product, **13**, had 1.6 D at position 2, 1.0 D each at positions 3 and 4, and 0.7 D at position 8. The deuterium on the nitrogen atom (N-D) is readily exchanged because of traces of water in the sample preparation procedures for both the GC-EIMS and NMR analyses.

The high-field ^1H NMR spectrum at 400 MHz also provided information concerning the stereochemistry of deuterium atoms at positions 3 and 4. The linewidths for multiplets at 1.90 ppm, assigned to H-3, and 2.73 ppm, assigned to H-4, were both 12.1 Hz, clearly indicative of a *cis* configuration[10] for the hydrogens on carbons 3 and 4[3,5–6] (Eq. (1)), i.e., a 3,4-*cis*-deuteration of the 3,4-double bond.[11] More important, when compound **12** was subjected to the same deuteration condition shown in Eq. (1), no exchange of the hydrogen atoms in the saturated nitrogen ring was observed by 250 MHz ^1H NMR spectroscopy. However, exchange of the aromatic hydrogen (position 8) that is beta to the nitrogen readily occurs with incorporation of 0.7 D, as evidenced by the decrease in the area of the doublet at 6.42 ppm, assigned to the proton on C-8 of compound **14** (Eq. (2)).

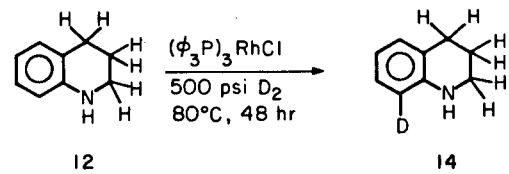

(2)

The experiment defined in Eq. (1) also showed by GC-EIMS that the remaining quinoline (~2%) was monodeuterated [$M^{+\cdot}$, *m/e* 130 (100% RA)]. Furthermore, if the reduction of **1** with deuterium gas (Eq. (1)) was allowed to proceed to only a 50% conversion of the deuterated tetrahydroquinoline, the remaining isolated **1** had deuterium incorporation exclusively at C-2, as evidenced by its 250 MHz ^1H NMR spectrum (8.9 ppm, doublet of doublets, 0.3 D). A GC-EIMS analysis showed a *m/e* 130 ion for quinoline-2-d, but in approximately 10% relative abundance. This strongly implies that the second deuterium incorporation at C-2, (i.e., **13**) comes predominately, but not exclusively, by deuteration of quinoline-2-d. This is substantiated by GC-EIMS and NMR analyses of the deuterated tetrahydroquinoline formed in the incomplete reduction (~50%), which indicates mainly 1,2,3,4-tetrahydroquinoline-d_3 rather than the d_4 compounds formed in the quantitative conversion, i.e., one deuterium at C-2 rather than 1.6 D.

Plausible Mechanistic Pathways in the Hydrogenation of Quinoline (1)

The deuterium results described above can be accommodated by several plausible rhodium intermediates, as shown in Fig. 3. Intermediate **B** can occur via intramolecular addition of deuterium (or hydrogen) to the carbon-nitrogen double bond via intermediate **A**. Exchange of the hydrogen on the

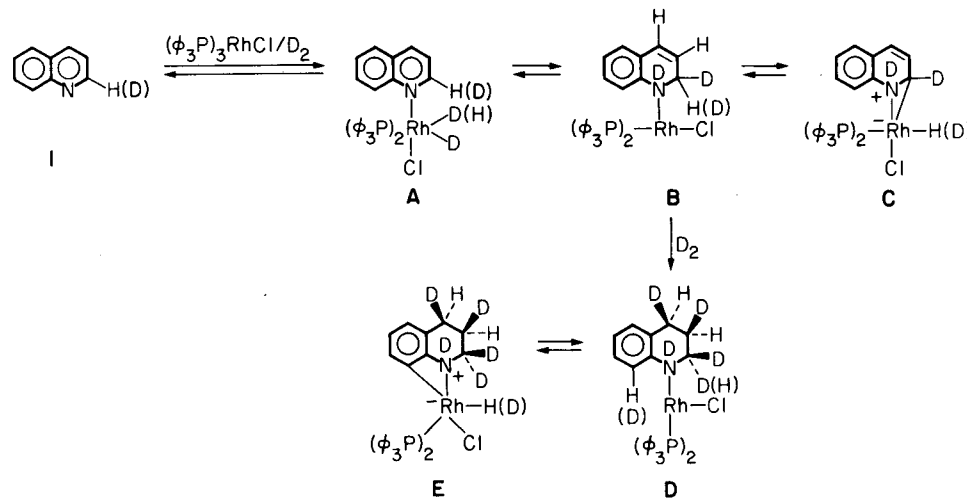

Figure 3. Plausible rhodium complexes as intermediates in the catalytic hydrogenation of quinoline, **1**.
(XBL 836-10433)

carbon that is alpha to nitrogen and allylic to the 3,4 double bond could occur by two pathways: (1) oxidative addition (cyclometallation) to give **C**; or (2) the apparently more predominate mechanism whereby intermediate **B** exchanges hydrogen for deuterium by being in equilibrium with **A** and quinoline-2-d. The latter compound can then recycle to **B**. Reduction of the 3,4 double bond may have a rate comparable to the dehydrogenation step, i.e., **B** → **A** → **1**, but it effectively eliminates any exchange at position 2. The cyclometallation reaction (oxidative addition) at position 8 (intermediate **E**) allows the exchange of that aromatic hydrogen.

Intermediates **C** and **E** (Fig. 3) have some precedents in the literature. For example, Bennett *et al.*[12] and Bruce, Goddall, and Stone[13] have reported on several ortho-metallation reactions with osonium and ruthenium carbonyls and compound **3** (Fig. 1) to provide the five-membered ring equivalent to intermediate **E** (Fig. 3). Yin and Deeming[14] have observed metallation of carbon atoms alpha to a nitrogen atom in several aromatic imine (ϕ-C=N-) derivatives. Crawford and Kaesz[15] and Crawford, Knobler, and Kaesz[16] have reported on a cyclometallated product, which had a metallo-azacyclopropane structure, as established by single-crystal x-ray crystallography, and represents a model for intermediate **C**. Laine *et al.*[17] have also postulated these metallo-azacyclopropane intermediates in deuterium exchange reactions with trialkylamine compounds as substrates and rhodium cluster carbonyls as catalysts.[17] The homogeneous catalytic activation of C-H bonds for hydrogen-deuterium exchange has been reviewed extensively by Parshall[18] and by Dehand and Pfeiffer.[19]

Dehydrogenation Step in Hydrogenation of 5

In experiments to provide more support for the dehydrogenation sequence, **B** → **A** → **1** (Fig. 3), we studied the deuteration of phenanthridine, compound **5**, and found, by GC-EIMS (*m/e* 184 32% RA) and 250 MHz ^{1}H NMR spectroscopy, two deuteriums at position 9 (absence of NMR signal at 4.4 ppm, singlet) and approximately 0.3 D at position 1 (7.66 ppm doublet) for compound **15**. Again, as in the deuterium gas experiments with **1**, the N-D group gets exchanged to some extent upon work-up (Eq. (3)).

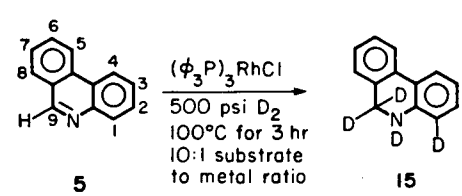

(3)

This result supports the hypothesis that activation of hydrogen on the carbon atom alpha to the nitrogen atom is a prerequisite for exchange, i.e., benzylic or allylic carbon positions. Furthermore, reaction of compound **15** with catalytic amounts of $(\phi_3P)_3RhCl$ readily provided the dehydrogenated product (25°C, 1 hour), phenanthridine-d_2 with deuteriums at the 9 and 2 positions as determined by

GC-EIMS and 250 MHz ^{1}H NMR spectroscopy (absence of singlet at 9.3 ppm assigned to the proton on carbon 9).

These results show that the dehydrogenation step by a plausible intermediate such as **B** to deuterated **1**, possibly via intermediate **A**, definitely occurs under the hydrogenation conditions.[20] The isolation of complexes such as **A-E** would obviously help our understanding of these rather complicated hydrogenation reactions, and such isolation studies are under way.

Summary

Although our results show the mechanistic complexities of hydrogenation in polynuclear heteroaromatic nitrogen compounds, several plausible reaction pathways have also been elucidated. The reduction of the carbon-nitrogen double bond, i.e., **1, 2, 3,** and **5**, is the initial product of hydrogen transfer from rhodium to the complexed substrate. This is followed by a reversible dehydrogenation step, as proved by deuterium experiments with **1** and **5**, a step that must have a rate comparable to the stereospecific reduction of the 3,4 double bond in compounds such as **1–3**. However, in the hydrogenation of compounds such as **5**, the metal-catalyzed dehydrogenation step must be extremely facile because of the benzilic nature of the methylene group that is alpha to the nitrogen atom. In addition, cyclometallation reactions may play a role not only in the exchange of aromatic hydrogens[12,13] but conceivably also in the exchange of hydrogens on the carbon alpha to the nitrogen.

It was also observed that both steric and electronic effects control the hydrogenation rates of our substrates in the presence of compounds that can competitively bind to the rhodium metal center. Knowledge of these effects should be highly useful in attempting to define the reactivity of these model coal compounds in very complex matrices such as coal liquids and shale oils.

PLANNED ACTIVITIES FOR FY 1984

We have carried out similar hydrogenation experiments with substrates **1–6**, using the heterogenized form of Wilkinson's catalyst, bonded to phosphinated polystyrene-divinylbenzene (2% or 20% crosslinked, 1–2% loading), and have found the same regioselectivity and excellent product conversions that we observed in the present study.[21] Subsequent manuscripts will detail catalytic-transfer hydrogenation results that exploit metal-catalyzed dehydrogenation of 9,10-dihydrophenanthridine.[22,23]

REFERENCES

1. Fish, R.H., Thormodsen, A.D., and Cremer, G.A. (1982), *J. Am. Chem. Soc. 104,* p. 5234.
2. Fish, R.H. (1984), *Ann. N.Y. Acad. Sci.*, in press.
3. Osborn, J.A., Jardine, F.H., Young, J.F., and Wilkinson, G. (1966), *J. Chem. Soc. A,* p. 1711.
4. Jardine, F.H., Osborn, J.A., and Wilkinson, G. (1967), *J. Chem. Soc, A,* p. 1574.
5. McQuillin, F.J. (1976), in *Homogeneous Hydrogenation in Organic Chemistry,* D. Reidel Publishing Co., Dordrecht, Netherlands, and references therein.
6. James, B.R. (1973), in *Homogeneous Hydrogenation,* Wiley, New York, and references therein.
7. A preliminary account was presented at the 3rd International Symposium on Homogeneous Catalysis, Milano, Italy, Aug. 30–Sept. 3, 1982, Abstract C33, p. 105; the Pacific Conference on Chemistry and Spectroscopy, San Francisco, CA, Oct. 27–29, 1983, Abstract 208, p. 96; and the New York Academy of Sciences Conference on Catalytic Transition-Metal Hydrides, New York, NY, November 15–17, 1982, Abstract 24.
8. Several examples of inhibition of olefin hydrogenation by pyridine and other coordinating substrates have been reported; see Candlin, J.P, and Oldham, A.R. (1968), *Discuss. Faraday Soc. 46,* p. 60, and Ref. 3.
9. Tolman, G.A. (1970), *J. Am. Chem. Soc. 92,* p. 2956.
10. Fish R.H. and Broline, B.M. (1978), *J. Organometal. Chem. 159,* p. 255.
11. For several examples of *cis* addition of deuterium to olefins using Wilkinson's catalyst, see: St. Jacques, M., and Prud'homme, R. (1970), *Tetrahedron Lett.*, p. 4833; Slack, D. and Baird, M.C. (1974), *J. Chem. Soc. Chem. Commun.*, p. 701; Gaghaire, and Voltero, P. (1970), *Bull. Soc. Chem. France,* p. 164; Hussey, A.S. and Takeuchi, Y. (1970), *J. Org. Chem. 35,* p. 643; and Refs. 3 and 6, p. 220.
12. Bennett, R.L., Bruce, M.I., Goddall, B.L., Iqbal, M.Z., and Stone, F.G.A. (1972), *J. Chem. Soc. Dalton,* p. 1778.
13. Bruce, M.I., Goddall, B.L., and Stone, F.G.A. (1973), *J. Organometal. Chem. 60,* p. 343.
14. Yin, C.C. and Deeming, A.J. (1977), *J. Organometal. Chem. 133,* p. 123 and references therein.
15. Crawford, S.S. and Kaesz, H.D. (1977), *Inorg. Chem. 16,* p. 3193.

16. Crawford, S.S., Knobler, C.B., and Kaesz, H.D. (1977), *Inorg. Chem. 16*, p. 3201.
17. Laine, R.M., Thomas, D.W., Carey, L.W., and Buttrill, S.E. (1975), *J. Am. Chem. Soc. 100*, p. 6527.
18. Parshall, G.W. (1975), *Acc. Chem. Res. 8*, p. 113.
19. Dehand, J., and Pfeiffer, M. (1976), *Coord. Chem. Rev. 18*, p. 327.
20. For a review of isomerization (dehydrogenation) of olefins under H_2 or D_2 conditions with rhodium catalysts see Ref. 5, Chap. 11, p. 198.
21. Fish, R.H., Thormodsen, A.D., and Heinemann, H. (1983), submitted to *Organometallics.*
22. Fish, R.H., Thormodsen, A.D., and Ausban, A. (1983), in preparation.
23. Fish, R.H., and Thormodsen, A.D. (1983), submitted to *Organometallics*, LBL-15596.

A Comparison of Polymer-Supported Wilkinson's Catalyst with Its Homogeneous Analogue in the Selective Reduction of Polynuclear Heteroaromatic Compounds*

R.H. Fish, A.D. Thormodsen, M. Simmons, and H. Heinemann[†]

Recently, we found that a wide variety of transition-metal compounds catalyzed the regiospecific reduction of polynuclear heteroaromatic nitrogen and sulfur compounds.[1–3] These findings may yield important improvements in synthetic fuel processes. Hydrogen gas consumption is known to be an economically limiting factor in the upgrading of synthetic fuels and in the removal of nitrogen and sulfur from these complex matrices. Selective hydrogenation would lower hydrogen consumption; furthermore, the reactions described here are carried out at lower temperatures and pressures than those used in conventional industrial processing.

Homogeneous catalysts have their own limitations, however. Recovery is often difficult or impossible. In addition, thermal stability and solubility may present problems in practical applications. The use of polymer supports, such as cross-linked polystyrene-divinylbenzene (PS-DVB), silica, and alumina to anchor homogeneous transition-metal catalysts and overcome some of these difficulties has been the subject of intensive research over the past 15 years. (For pertinent reviews and leading publications, see Refs. 4–7.)

In this article, we compare some initial results for Wilkinson's catalyst supported on 2% cross-linked phosphinated PS-DVB with those for its homogeneous analogue[2] in selectively reducing polynuclear heteroaromatic nitrogen and sulfur compounds (Fig. 1).

ACCOMPLISHMENTS DURING FY 1983

Initial and Relative Rates

The initial and relative rates of reduction of the substrates **1–5** (Fig. 1) were obtained using a Parr kinetic apparatus[2]; Table 1 lists the results. Substrate-to-metal ratio, temperature, and partial

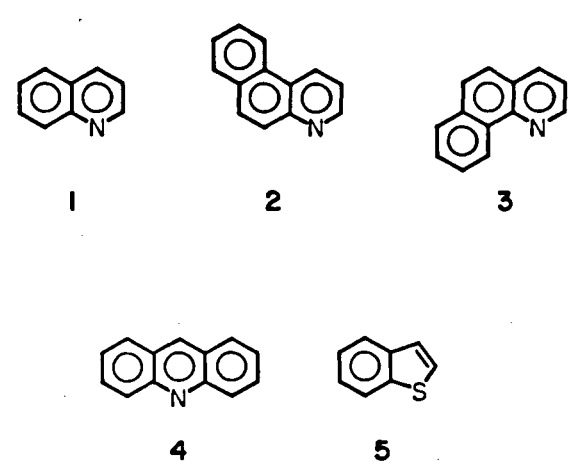

Figure 1. Polynuclear heteroaromatic compounds used as substrates for reduction studies: **1**, quinoline; **2**, 5,6-benzoquinoline; **3**, 7,8-benzoquinoline; **4**, acridine; **5**, benzothiophene. (XBL 8311–4462)

*This work was jointly supported by the Director, Office of Energy Research, Office of Basic Energy Sciences, Chemical Sciences Division, and the Assistant Secretary of Fossil Energy, Office of Coal Research, Liquefaction Division of the U.S. Department of Energy, the Pittsburgh Energy Technology Center, and the Electric Power Research Institute through the Department of Energy under Contract No. DE-AC03-76SF00098.

[†]Materials and Molecular Research Division.

Table 1. Comparison of initial and relative rates of hydrogenation of substrates **1–5** using both polymer-supported and homogeneous Wilkinson's catalyst.[a]

		Polymer-supported rates[c]		Homogeneous rates		
Substrate	Product[b]	Initial (%/min)	Relative	Initial (%/min)	Relative	PS/H rate ratio
1, Quinoline	1,2,3,4-Tetrahydro-	0.29	1	0.013	1	22
2, 5,6-Benzoquinoline	1,2,3,4-Tetrahydro-	0.14	0.48	0.0065	0.5	22
3, 7,8-Benzoquinoline	1,2,3,4-Tetrahydro-	0.024	0.08	0.0012	0.09	20
4, Acridine	9,10-Dihydro-	~0.4	~1.4	~0.04	~3	10
4, Acridine	1,2,3,4-Tetrahydro-	0	0	0.047	3.6	0
5, Benzothiophene	2,3-Dihydro-	~0.03	~0.1	0.044	3.4	0.7

[a] Reaction conditions were as follows: P_{H2} = 310 psi, T = 85°C, sub./cat. = 91/1, benzene (20 mL), 1 mmole substrate in each case, with either 10.2 mg of homogeneous $RhCl(PPh_3)_3$ or 52 mg of polymer-supported Wilkinson's catalyst [2% cross-linked, 2.19% Rh, initial P/Rh = 2.9 (Strem Chemical Co.), P/Rh after reaction with substrates **1–5** ~ 3.3]. The catalyst was contained in a wire basket attached to the end of the dip tube of the kinetic apparatus.

[b]Analysis by gas chromatography.

[c]Plots of % conversion vs. time provided initial (pseudo-zero order) rates. Rates are relative to quinoline (1.0). Substrates **1–5** were reacted with the same beads for all initial rates reported.

pressure of hydrogen were the same for both forms of Wilkinson's catalyst. Experiments with the polymer-supported catalyst were all carried out using the same batch of 2% PS-DVB beads, with excellent reproducibility.

Clearly, several important observations can be drawn from the results in Table 1. The table shows that the initial rates of hydrogenation of nitrogen heterocyclic compounds, **1–4**, with polymer-supported Wilkinson's catalyst are 10 to 20 times faster than with the homogeneous equivalent. This rate enhancement, which has not been observed with many polymer-supported catalysts in reduction reactions,[5,8] is extremely relevant for practical applications.

Several reasons for this favorable result can be formulated. Substrates **1–4** are themselves suitable ligands, and a higher concentration or enrichment of substrate around the polymer-supported metal center, with a concomitant loss of triphenylphosphine, may have enhanced the rates. Other factors, such as steric and electronic effects, are probably involved as well. The relative-rate differences among **1–5** for both forms of Wilkinson's catalyst may involve steric effects as accentuated by the 5,6- and 7,8-benzoquinoline (**2** and **3**) rate ratio, i.e., **2/3** = 6.0, as well as the ratios with **1**, i.e., **1/2** = 2, and **1/3** = 13. Only in the case of the sulfur heterocyclic compound, **5**, is the initial rate larger for the homogeneous catalyst, while overall relative rates are similar for **1–4** within each set of catalyst results.

Selectivity

The high regioselectivity for the heteroaromatic ring with both forms of the catalyst is evident (Table 1). In one case, substrate **4**, the polymer-supported catalyst gave only 9,10-dihydroacridine, with no 1,2,3,4-tetrahydroacridine apparent. In contrast, with the homogeneous analogue,[2] **4** gave substantial amounts of the outer ring product (~50%), and this difference may result from the more pronounced steric requirements surrounding the active metal sites on the polystyrene-divinylbenzene-supported catalyst.[4–7]

Parameters Affecting Rates

Other parameters that needed study included the effect of cross-linking and the diffusion rates of substrate into the PS-DVB beads. In experiments to clarify these points, the 2% cross-linked polystyrene-divinylbenzene beads with Wilkinson's catalyst were compared to the 20% cross-linked beads for reduction of **1**. The initial rate ratio for both (2%/20%)

was found to be approximately 3. We also ground the 2% beads and hydrogenated substrate **1** (quinoline), using similar reaction conditions, to show that diffusion of substrate into the bead was not rate limiting, i.e., both ground and whole (~30 μ) 2% cross-linked beads gave the same initial rates within experimental error.

Mechanism of Hydrogenation of 1 with Polymer-Supported Wilkinson's Catalyst

The mechanism of reduction of **1** with homogeneous Wilkinson's catalyst was recently elucidated with deuterium gas and is discussed elsewhere.[2] In that study, we found that deuterium was incorporated as shown in the following scheme for **6**:

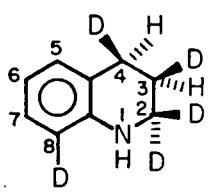

6

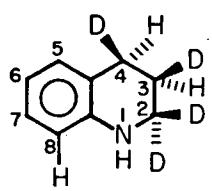

7

In contrast, compound **7**, above, shows the deuterium pattern (NMR and mass spectroscopy)[9] obtained with 2% cross-linked PS-DVB Wilkinson's catalyst. The pertinent difference is the lack of aromatic C-H exchange for the polymer-supported catalyst; stereochemistry at the 3,4 double bond *(cis)* and reversible dehydrogenation of the reduced carbon-nitrogen bond (positions 1 and 2) to provide 1.6 D at position 2, via quinoline-2-d, are similar for both forms of the catalyst. Moreover, reaction of the product, 1,2,3,4-tetrahydroquinoline, with PS-DVB Wilkinson's catalyst under similar deuteration conditions also shows, by NMR and MS analyses, no exchange of the aromatic hydrogen at position 8 (6.42 ppm), in contrast to the result for the homogeneous catalyst.[2] Again, steric requirements surrounding the active metal center of the polymer-supported catalyst may be responsible for the lack of aromatic C-H exchange.[5]

Reduction of 1 in the Presence of Model Coal Liquid Constituents

Since the compounds shown in Fig. 1 are prevalent in synthetic fuel products such as coal liquids, we wanted to determine whether selectivity for the nitrogen heterocyclic ring (with **1** as the example) would prevail in the presence of other coal-liquid constituents. We used a model coal liquid dissolved in benzene and containing (wt%) 30% pyrene, 5% tetralin, 38% methylnaphthalene, 17% m-cresol, 7.5% **1**, and 2.5% 2-methylpyridine.[10] The liquid was hydrogenated with the 2% PS-DVB Wilkinson's beads (under conditions similar to those in Table 1) to provide 1,2,3,4-tetrahydroquinoline as the only reduction product (initial rate 0.42%/min). Removal of 2-methylpyridine had no effect on the initial rate, in contrast to competitive inhibition on **1** by the pyridine derivative in the homogeneous reaction.[2] Interestingly, reduction of **1** alone, at a similar substrate-to-metal ratio as in the model coal liquid, provided an initial rate (0.18%/min) that was ~2.2 times slower than the rate of **1** in the presence of the model coal-liquid constituents.

PLANNED ACTIVITIES FOR FY 1984

The impressive result just cited emphasizes the highly selective reaction taking place in the presence of other functionalities, i.e., regiospecific reduction of the nitrogen heterocyclic ring as well as the rate enhancement phenomena, and provides dramatic evidence for the potential usefulness of polymer-supported catalysts in synthetic fuel (hydroprocessing) applications.[11] We will continue to pursue the use of these catalysts in model coal-liquid hydrogenation experiments.[12]

REFERENCES

1. Fish, R.H., Thormodsen, A.D., and Cremer, G.A. (1982), *J. Am. Chem. Soc. 104*, p. 5234.
2. Fish, R.H., and Thormodsen, A.D. (1983), submitted to *Organometallics.*
3. Fish, R.H. (1983), *Ann. N.Y. Acad. Sci.*, in press.
4. Bailar, J.C., Jr. (1974), *Catal. Rev. 10*, p. 17.
5. Hartley, F.R., and Vezey, P.N. (1977), *Adv. Organometal Chem. 15*, p. 189.
6. Whitehurst, D.D. (1980), *Chemtech*, p. 44.
7. Ciardelli, F., Braca, G., Carlini, C., Sbrana, G., and Valentini, G. (1982), *J. Mol. Cat. 14*, p. 1.
8. Pittman, C.U., Jr., Smith, R.J., and Hanes, R.M. (1975), *J. Am. Chem. Soc. 97*, p. 1742.
9. The ^{1}H 250 MHz NMR spectrum (benzene-d_6) for 1,2,3,4-tetrahydroquinoline-d_3 had signals at 1.90 (H-3); 2.73 (H-4); 3.24 (H-2); 6.42 (H-8); 6.55 (H-5); and 6.93 (H-1 and H-7) ppm with areas of 1:1:0.4:1:1:2, respectively, and EIMS data provided the *m/e* 136 ion.
10. This model coal liquid was suggested by Linda Atherton of the Electric Power Research Institute.

11. These results were presented at: New York Academy of Sciences Conference on Catalytic Transition Metal Hydrides, New York, NY, November 15–17, 1983; 1983 International Conference on Coal Science, Pittsburgh, PA, August 15–19, Eighth Annual EPRI Contractors on Coal Liquefaction, Palo Alto, CA, May 11–13, 1983; and in a poster session at the Fourth International Symposium on the Relations Between Homogeneous and Heterogeneous Catalysis, Asilomar, CA, October 2–5, 1983.
12. Fish, R.H., Thormodsen, A.D., and Heinemann, H. (1983), submitted to *Organometallics*, LBL-16918.

COAL-RELATED RESEARCH

Processing of Condensate Waters from Coal Gasification*

C.J. King, D. Mohr, P. MacKenzie, J. Senetar, J. Bixby, R. Demyanovich, and R. Thompson

Large volumes of condensate water are formed when reactor effluents from coal gasification are cooled. These water streams contain large concentrations of ammonia, acid gases, and dissolved organics—notably phenolic compounds. The degree of contamination is highest for lower-temperature gasification processes. For economic and environmental reasons, these waters must be processed for recycling, probably as make-up water for a cooling-tower system. The principal objective of this work is to develop workable, reliable, and economical physicochemical processing methods for such recycling and to provide underlying design data. Particular attention has been given to solvent-extraction and stripping processes and to analysis of the chemical composition of water samples.

Work to date has focused on four areas:

(1) analyses of individual components contributing to the measured chemical oxygen demand (COD);
(2) extraction with both conventional and novel solvents to effectively remove the COD and allow regeneration with low energy consumption;
(3) interpretation of rates of stripping of ammonia and acid gases such as CO_2 and H_2S from condensate waters; and
(4) combining extraction of ammonia with stripping of acid gases in an innovative process that can recover ammonia as a salable product.

*This work was supported by the Assistant Secretary for Fossil Energy, Office of Coal Utilization, Advanced Conversion and Gasification, Division of Surface Coal Gasification, of the U.S. Department of Energy, through the Morgantown Energy Technology Center, under Contract No. DE-AC03-76SF00098.

ACCOMPLISHMENTS DURING FY 1983

Analysis of Condensate Waters

The 1982 Annual Report described our detailed analyses of four water samples from the slagging fixed-bed gasifier at the Grand Forks Energy Technology Center (GFETC). The identified components, if their complete oxidation is assumed, accounted for 70% to 83% of the total measured COD. The measurements were made by high-performance liquid chromatography (HPLC), supplemented by gas chromatography/mass spectrometry (GC/MS) and a procedure of distillative solvent change from water to isopropanol.

Subsequent gas-chromatographic analyses with an 18-inch Porapak Q column and a flame-ionization detector have revealed 1000 ppm w/w of methanol, 500 ppm of acetone, and 280 ppm of acetonitrile in one of the GFETC samples (RA-106). This increases the fraction of COD identified from 69.9% to 83.9%, again assuming complete oxidation in the COD analysis. Acetone and acetonitrile would be expected to be stripped effectively from these waters, but methanol would not be. Furthermore, methanol is probably incompletely extracted with common solvents such as methyl isobutyl ketone (MIBK) and diisopropyl ether (DIPE) and so is probably a significant constituent of the COD remaining after extraction with such solvents.

Tests have been made of the degree of oxidation of various compounds in the COD analysis. Among the phenolic compounds, phenol, m-cresol, and 3,4-xylenol oxidized 99% to 100%, and o-cresol, p-cresol, 2,6-xylenol, and 3,5-xylenol oxidized 94%, 92%, 97%, and 93%, respectively. These results suggest that another 1% to 2% of the COD remains unidentified, beyond what is computed by assuming that the identified components oxidize completely.

Analyses have been made of the organic sulfur and organic nitrogen compounds in the samples, along with their extractability and volatility. For GFETC sample RA-106, 383 mg/L of organic sulfur was found, and for sample RA-120, 175 mg/L of organic nitrogen was found. A batch distillation of the stripped raffinate left after extraction of RA-106 with MIBK showed that 38% of the unextracted COD appeared in a 90% distillate fraction, while the remaining unextracted COD stayed with the 10%

bottoms fraction. A batch distillation of unextracted RA-106 showed that 97% of the organic sulfur remained in a 27% bottoms fraction. Extractions of this water at pH 2 with both MIBK and methylene chloride removed virtually none of the organic sulfur, but extractions at pH 9 removed 57% and 25%, respectively, of the organic sulfur. These results suggest that much of the organic sulfur protonates at low pH.

Batch distillation of the stripped raffinate from MIBK extraction of GFETC sample RA-120 showed that 42% of the unextracted COD and 3% of the unextracted organic nitrogen appeared in an 89% distillate fraction. Thus the organic nitrogen and organic sulfur compounds are relatively nonvolatile. Since distillation of this raffinate after adjustment to pH 12 gave essentially the same result, the low volatility is not the result of ionization of basic organic nitrogen compounds.

The concentration of SCN^- in RA-120 was found to be 45 mg/L. Since SCN^- responds to the organic nitrogen test, it accounts for about 5% of the measured organic nitrogen content.

A sample was also received from the Morgantown Energy Technology Center's (METC) gasifier run 101. An analysis of this water, made promptly upon receipt, is shown in Table 1.

One of our earlier accomplishments was the first identification of hydantoin compounds in condensate waters from coal conversion. This identification was made using distillative solvent transfer from water to isopropanol, followed by GC/MS analysis using electron ionization. We have since confirmed the identification using GC/MS with chemical ionization (methane), and independent identifications of hydantoins in condensate waters from coal gasification have been made at GFETC and METC.

A likely candidate for the formation reaction of 5,5-dimethyl hydantoin (DMH) in the aqueous phase is the Bucherer-Bergs reaction, which produces DMH and water stoichiometrically from acetone, ammonia, carbon dioxide, and hydrogen cyanide.

Table 1. Analysis of condensate water from Morgantown Energy Technology Center gasifier run 101.

Compound	Concentration (mg/L)	COD[a] (mg/L)	% of Measured COD
Phenol	1380	3920	26.3
Cresols	1990	5000	39.9
Xylenols	840	2210	17.7
o-Methoxyphenol	b		
o-Hydroxyacetophenone	b		
Pyrocatechol	40	80	0.6
4-Methylpyrocatechol	40	80	0.6
Resorcinol	65	125	1.0
Hydroquinone	4	8	0.1
5,5-Dimethyl hydantoin (DMH)	20	21	0.2
Acetonitril	65	98	0.8
Acetone	60	125	1.0
Methanol	b		
TOTAL		11040	88.2
Measured COD		12520	
Organic nitrogen	93		
Organic sulfur	60		

[a]Assuming 100% oxidation.

[b]Concentration essentially zero.

This is consistent with observed differences of −1.97 m*M*/L and +1.79 m*M*/L for concentrations of acetone and DMH, respectively, between samples of RA-106 condensate water stored at pH 2 and pH 9. The hydantoin-forming reaction is effectively stopped in the low-pH water.

Finally, the pK_a of DMH was estimated at 8.9 from a measurement of the pH of the compound dissolved in Milli-Q purified distilled water. From extraction-equilibrium data, the value of pK_a was estimated at 9.0 to 9.1. Therefore, this compound can be partially dissociated in typical condensate waters.

Research on analysis of the GFETC condensate waters is described in more detail elsewhere.[1-3]

Extraction with Trioctyl Phosphine Oxide

Results obtained for extraction of GFETC condensate waters with conventional solvents such as MIBK, diisopropyl ether, and tributyl phosphate have been described in previous Annual Reports and elsewhere.[2,3]

Trioctyl phosphine oxide (TOPO) has been found in our earlier work to be a particularly effective extractant for phenols.[4] Subsequent research[5] has sought to find effective diluents that would allow regeneration by distilling phenol overhead. The hydrogen-bonded complex between phenol and TOPO is still strong at the atmospheric boiling point of phenol (182°C), so it is necessary to use dilutents with substantially higher boiling points. A series of experiments using a vapor-liquid equilibrium still demonstrated that hydrocarbon diluents boiling at about 260°C are effective. One suitable mixture combines dimethyl naphthalene (for solubility of TOPO) and n-octadecane (for density control). Commercial hydrocarbon/solvent mixtures can be blended to give similar characteristics. Measurements of extraction equilibria for removal of phenol from water using solvents composed of TOPO, dimethylnaphthalene, and octadecane showed that the change of diluent from the previously used diisobutyl ketone causes relatively little change in the extraction equilibria.

Back-extraction of solutes into solutions of strong aqueous bases can be an effective means of regeneration if conversion of acid solutes to salts can be accepted. In the case of TOPO-based solvents, back-extraction of this sort is complicated by emulsion formation. Tests have shown that this tendency is reduced if the aqueous phase used for regeneration has both a high pH and a high ionic strength.

Phase-Splitting Extraction

Certain extraction agents afford the possibility of separation through a temperature change, taking advantage of large changes in phase miscibility with changing temperature. One such reagent, "glyeth," the diethyl ester of ethylene glycol, was used to extract a solution of 1.0% phenol, 12.1% ammonium bicarbonate, and 2.54% ammonium carbonate in water (pH = 8.36), at a volumetric phase ratio of about 1:1 and a temperature of 225°C, under pressure. It was hoped that the inorganic salts would remain largely in a highly concentrated aqueous phase, while the phenol and much of the water extracted largely to the organic phase, thereby giving a preliminary separation of organics from inorganics and concentrating the inorganics. It was found that the aqueous and organic phases contained 6.77% and 1.46% ammonium carbonate and bicarbonate (expressed as the carbonate), respectively. Phenol split very evenly between the phases. The separation selectivity of this method appears to be limited.

Combined Stripping and Extraction for Removal and Isolation of Ammonia[6]

This effort explores methods of recovering and isolating ammonia through combined solvent extraction and stripping. In conventional stripping of ammonia and acid gases, the steam requirement is large because the volatilities of the solutes are highly suppressed by ionization in solution. Extracting ammonia shifts the pH to lower values, increasing the volatilities of acid-gas solutes and thereby lessening the steam requirements for stripping them from the solution. Such a process also serves to isolate ammonia as a separate, salable product. One possible version of this process is shown in Fig. 1.

In earlier work, we showed that liquid cation exchangers are most effective for extraction of ammonia, because they interact directly with ammonium ion. For degree of extraction, regenerability, and thermal stability, di-2-ethylhexyl phosphoric acid (D2EHPA) has been found to be an attractive liquid cation exchanger. It is commonly used in hydrometallurgical processing.

Various diluents have been explored for use with D2EHPA. Aromatics give lower aqueous losses of D2EHPA, better phase-settling properties, and a lower degree of ammonia extraction than aliphatic diluents. To enhance these properties, it is desirable to add modifiers, or third components, to the solvent mixture. Unhindered alcohols, phenols, and carboxylic acids increase the degree of ammonia extraction, reduce losses of D2EHPA to the aqueous phase,

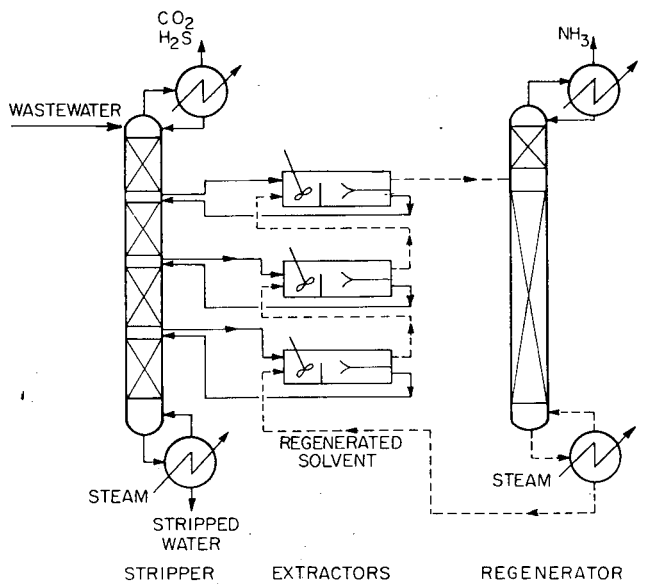

Figure 1. Schematic of a possible process to isolate ammonia from condensate waters by solvent extraction and steam stripping. (XBL 838–534)

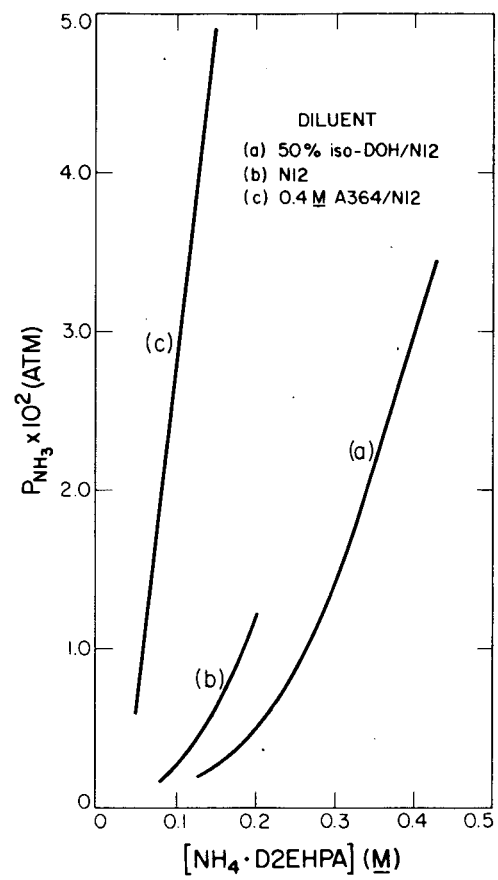

Figure 2. Batch-regeneration data for solvents containing D2EHPA and one of three diluents, plotted against partial pressure of ammonia. Total D2EHPA concentration for each diluent: (a) 0.48 *M*; (b) 0.48 *M*; (c) 0.4 *M*. Temperature: 127°C. (XBL 838–538)

and improve phase-separation properties. These results suggest that these modifiers solvate both D2EHPA and the D2EHPA/ammonium-ion pair, but the latter more strongly. A tertiary amine modifier (e.g., Adogen 364, Sherex Division, Ashland Chemicals) lowers the degree of extraction of ammonia, reduces losses of D2EHPA to the aqueous phase, and improves phase separation. These results indicate that the amine interacts strongly with D2EHPA and may also offer some solvation to the ion pair.

Detailed measurements of equilibrium distribution coefficients for NH_3 have been made for toluene, a mixture of toluene and isodecanol, and mixed toluene and Adogen 364 as diluents for D2EHPA. The results have been interpreted in terms of models allowing for formation of the ion pair and further complexation of the ion pair by additional D2EHPA.

Figure 2 shows data taken during batch regeneration of solvents containing D2EHPA, various stoichiometric loadings of ammonia, and one each of the three diluent systems studied. The hydrocarbon constituent of each diluent is Norpar 12 (C_{11} to C_{13} normal paraffins, King Industries). The diluent mixtures are (a) 50% isodecanol in Norpar 12, (b) pure Norpar 12, and (c) 0.4 *M* Adogen 364 in Norpar 12. The partial pressures of ammonia are calculated from the observed rates of stripping of ammonia by nitrogen passed through the solutions at 127°C. Adding alcohol to the diluent *decreases* the volatility of ammonia for a given NH_3/D2EHPA stoichiometry, because of the added solvation of the ion pair by the alcohol. Adding amine to the diluent *increases* the volatility of the ammonia, because the amine competes with the ammonia for formation of ion pairs with D2EHPA.

Figure 3 shows rates of stripping of carbon dioxide by nitrogen from aqueous solutions containing NH_3 and CO_2, with and without added solvent mixtures. The rate of stripping of CO_2 is much greater in the presence of the D2EHPA-containing solvents. In all cases with the solvents present, less than 1.0% of the ammonia was stripped, because of the extraction of NH_3 into the solvent phase. Consistent with the other results, addition of an alcohol (Alfol 10, Conoco Chemical Co.) increased the rate of CO_2 stripping because of greater NH_3 extraction, and addition of Adogen 364 decreased the rate because of lesser NH_3 extraction.

A computer model of the volatilities of CO_2 and NH_3 above solution was used to analyze steam

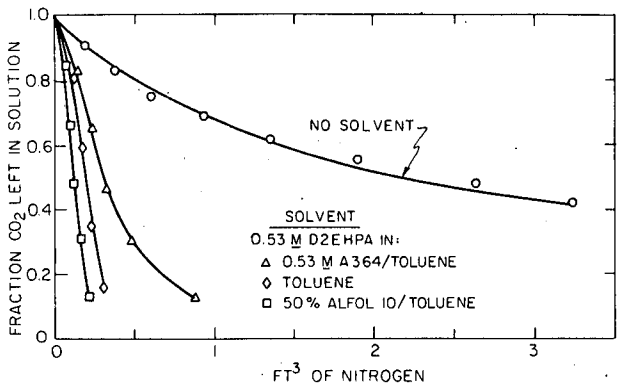

Figure 3. Rates of stripping of CO_2 by nitrogen from aqueous solutions of NH_3 and CO_2, with and without D2EHPA solvent mixtures. (XBL 8311-6571)

requirements for the CO_2 stripper in the process shown in Fig. 1. For a feed containing 1.0% NH_3, with a solvent composed of 0.5 *M* D2EHPA and 0.25 *M* Adogen 364 in a C_{11} alkane diluent, with a volumetric solvent/water ratio of 2.5, the CO_2 stripper would require 0.09 lb steam/lb feed water; the solvent regenerator—operating under vacuum—would require 0.05 lb steam/lb feed water, and the NH_3/H_2O fractionator would require 0.04 lb steam/lb feed water. Thus the total steam requirement would be 0.18 lb/lb feed water. This compares favorably with the steam requirements of other processes that isolate ammonia from sour waters. The U.S. Steel Phosam-W and Chevron all-distillation processes consume between 0.25 and 0.35 lb steam/lb feed water for similar feeds. The amine modifier therefore appears to be desirable for keeping the regenerator steam requirement low.

Synfuels Wastewater Workshop

Members of the project team worked with METC personnel to organize and conduct a Synfuels Wastewater Workshop for DOE contractors and other invited persons, and to edit the proceedings. The workshop was held in Morgantown, West Virginia, on June 15–16, 1983.

PLANNED ACTIVITIES FOR FY 1984

Analyses of condensate waters from the METC gasifier and any other available sources will be continued to identify the principal contributors to the as-yet unidentified COD, as well as any important classes of organic compounds that have not previously been reported. Methods used will include mass spectrometry, GC/MS, solvent-change techniques, HPLC, GC, and various generic techniques (organic nitrogen, organic sulfur, etc.). Efforts will be made to identify the organic nitrogen and organic sulfur compounds, and to identify any amphoteric substances (e.g., amino acids). For these purposes, pH-gradient HPLC will be employed.

Studies of processing techniques will be directed toward solvent extraction (both single and successive solvents), stripping, adsorption with various adsorbents, and evaporation. Favorable combinations of these processes will also be sought. Much of the as-yet unidentified COD has proved difficult to remove by conventional biological and physiochemical techniques. More effective means for removing these substances will be sought.

A new component of the project will be directed toward formation and removal of hydantoin compounds. The formation reactions will be better identified and confirmed, and the kinetics of these reactions in aqueous solution as functions of pH, temperature, and composition will be monitored. Among the removal techniques to be investigated are extraction with various solvents, including ion-pair extraction, and adsorption onto carbons and resins with particular functional groups.

Design parameters for simultaneous extraction and stripping for recovery and isolation of ammonia will be characterized and compared more thoroughly with conventional stripping and with the Phosam-W and all-distillation processes. Simultaneous extraction of organics will also be characterized, with an eye to identifying resultant problems and/or possibilities for synergism with other methods of removing organics.

REFERENCES

1. Mohr, D.H., Jr., and King, C.J. (1983), *Identification and Separation of the Organic Compounds in Coal-Gasification Condensate Waters,* Ph.D. dissertation, University of California, Berkeley; LBL-15869.
2. Mohr, D.H., Jr., Senetar, J.J., and King, C.J. (1983), "Characterization of GFETC Coal-Gasification Condensate Waters," presented at the Synfuels Wastewater Workshop, Morgantown, WV, June 15–16, 1983; LBL-16160.
3. Mohr, D.H., Jr., and King, C.J. (1983), "Solvents for Bulk Removal of Organics from Coal-Conversion Condensate Waters," in *Proceedings of the International Solvent Extraction Conference* (ISEC'83), Denver, CO, August 26–September 2, 1983; American Institute of Chemical Engineers.
4. MacGlashan, J.D., and King, C.J. (1982), "Extraction of Phenols from Water with Trioc-

tyl Phosphine Oxide," M.S. thesis, University of California, Berkeley; LBL-13963.
5. Bixby, J.L., and King, C.J. (1983), "The Regeneration of Trioctyl Phosphine Oxide Solutions Used to Extract Phenol from Water," M.S. thesis, University of California, Berkeley; LBL-16577.
6. Mackenzie, P.D., and King, C.J. (1983), "Simultaneous Stripping and Extraction for Recovery of Ammonia from Sour Water," in *Proceedings of the International Solvent Extraction Conference* (ISEC'83), Denver, CO, August 26–September 2, 1983, American Institute of Chemical Engineers, LBL-15828.

Enhancing Efficiency in Dry-Ash Moving-Bed Gasifiers Through a Distributed Feed*

C.H. Lu[†] *and M.M. Denn*

The overall efficiency of the conventional pressurized moving-bed technique of coal gasification is limited by the need to add large amounts of excess steam to keep the solids temperature below the softening point of the ash. The Lurgi dry-ash reactor, for example, which has been in commercial use since 1936, typically uses 7 to 9 moles of steam for each mole of oxygen with a feed of pure oxygen, and 5 to 7 moles of steam for each mole of oxygen with an air feed, whereas a steam-to-oxygen mole ratio close to unity is desirable.[1,2] The resolution within the context of moving-bed technology has been the development of the slagging reactor, which operates at a low steam-to-oxygen ratio (approximately unity) and at a sufficiently high temperature to cause the ash to form a molten slag. The British Gas/Lurgi slagger is described by Sharman and Scott.[3] This reactor has not reached commercial status, although these authors conclude that it "can now be regarded as ready for commercial exploitation" and that it is "particularly suitable for high volatile, unreactive, bituminous coals."

The high temperatures in the slagger can be a source of materials and operating problems. Work on moving-bed reactor modeling[4–7] has led to an alternative concept in which the low-temperature operation of the dry ash reactor is maintained, but with a low steam-to-oxygen ratio. The basic approach, first investigated by Denn *et al.*,[8] is to feed only part of the oxygen at the reactor bottom and to distribute the remainder axially in order to broaden the partial combustion zone.

This article describes simulations indicating that the approach is feasible in principle and could lead to a highly efficient dry-ash reactor for low reactivity coal. The engineering problems involved are also discussed briefly.

ACCOMPLISHMENTS DURING FY 1983

Model

The reactor model used in our calculations is a modification of the one-dimensional, homogeneous model described by Yoon *et al.*[5,6]; this model predicts reactor effluents that are in agreement with plant data and maximum temperatures in the operable range for the feed conditions used in the plant tests. Yoon's model is based on detailed mass and energy balances and includes mass transfer and kinetic limitations. Mass-action kinetics are assumed for the intrinsic reaction rates of the heterogeneous combustion and gasification reactions. The only adjustable parameter in the model is the CO/CO_2 selectivity of carbon oxidation, which is not well-established under gasifier conditions. The gas is assumed to be in plug flow, and radial variations in concentrations and temperature are not considered. Calculations based on a two-dimensional model[4,7] show that the assumption of adiabatic operation with radial uniformity is a good approximation over most of the cross section when operating near the design throughput.

The only modification we have made to this basic model is to add source terms to account for gaseous feeds along the length of the reactor. The gas is assumed to be distributed over the reactor cross section at any feed point without disturbing the axial plug flow or the radial uniformity of concentrations and temperature. The computer code differs from Yoon's (which is available from EPRI) because

*This work was supported by Lawrence Berkeley Laboratory Program Development Funds and by the Assistant Secretary of Fossil Energy, Office of Surface Coal Gasification, Division of Coal Projects Management of the U.S. Department of Energy under Contract No. DE-AC03-76SF00098.

[†]Present Address: Beijing Research Institute of Coal Chemistry, Beijing, China.

of the need to normalize fluxes on a different basis, but the structure is similar. The differential equations are solved using the Runge-Kutta-Boone method, which is adequate, despite the steep temperature gradients.

All calculations were carried out for an air-blown gasifier converting 120 lb/hr/ft^2 of fixed carbon, corresponding to approximately 233 lb/hr/ft^2 of dry coal, at 350 psig and a blast temperature of 700°F. The coals were assumed to have the properties of Illinois No. 6 bituminous and Wyoming subbituminous coal, with physical parameters and reactivities as given by Yoon *et al.*[8] The Illinois and Wyoming coals are typical low- and high-reactivity U.S. coals, respectively. The gasifier height was taken to be 10 feet.

Operating Limits

A constraint upon the gasifier is that it must operate within a fixed maximum temperature. In a bottom-fed gasifier, this maximum temperature is determined by the solution of an initial-value problem in which steam and oxygen fluxes and residual carbon in the ash are specified. Feed conditions corresponding to a maximum temperature of 2090°F for the Illinois coal with air as the oxidant are shown in Fig. 1. The dashed line is the locus of points along which the carbon material balance is satisfied exactly at the top of the reaction zone. Points above this line are inadmissible because they would require more than 100% of the feed carbon at the top. The right-hand corner of the feasible region, with oxygen and steam fluxes of 114 and 429 lb/hr/ft^2, respectively, corresponds to the optimal operating point reported by Yoon *et al.*[9] A similar graph has been

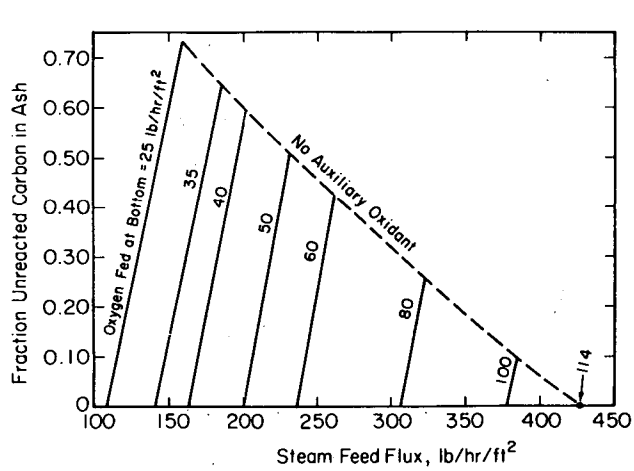

Figure 1. Conditions at the reactor bottom corresponding to a maximum temperature of 2090°F with Illinois No. 6 coal. (XBL 8312–4336)

constructed for the Wyoming coal, using a maximum temperature of 2140°F.

Operating conditions having only a small amount of carbon in the ash are defined by the intersections of the lines of constant oxygen flux with a specified amount of unreacted carbon (equal to 0.01% in our calculations); this fixes the oxygen, steam, and carbon fluxes at the bottom, and hence the position of the maximum temperature. When the maximum temperature has been reached, it is necessary to add oxidant according to some spatial program that leads to satisfaction of the carbon material balance at the top of the reaction zone. For example, Denn *et al.*[8] used a constant rate; in this case, there are two parameters to be determined by iterative calculation: the oxidant feed rate and the corresponding length of the auxiliary oxidation zone. The feed rate is limited by the maximum-temperature constraint.

It appears to be more efficient to program the oxidant feed so that the system operates autothermally at the maximum permissible temperature, since this mode of operation will maximize the gasification rates. The feed rate can be approximated by assuming that oxidation is instantaneous and that all of the oxidation reaction enthalpy change is utilized for steam gasification, followed by water-gas shift equilibrium. The gasification rate, and hence the required reaction enthalpy change, is fixed by the temperature and the gas composition, so the oxidation feed rate is therefore fixed. The feed rate can be adjusted to maintain a constant temperature following this first approximation, but the procedure outlined here to calculate a point flux at the start of every second integration step was adequate to maintain the maximum temperature constant to within 5°F without iteration. The required length of the feed zone to satisfy the carbon material balance is then found by iteration. A typical oxygen feed distribution is shown in Fig. 2, corresponding to a steam feed flux of 163.2 lb/hr/ft^2 and an oxygen flux at the bottom of 40 lb/hr/ft^2 to ignite the reaction.

Results

The required oxygen feed flux as a function of steam flux is shown in Fig. 3 for the Illinois coal (maximum operating temperature, 2090°F); a similar chart has been constructed for the Wyoming coal (maximum operating temperature, 2140°F). There is a fourfold decrease in the steam requirement for the Illinois coal and a twofold decrease for the Wyoming coal. The total oxygen feed to the reactor is reduced by about 20% because less undecomposed steam must be heated from the blast temperature to the

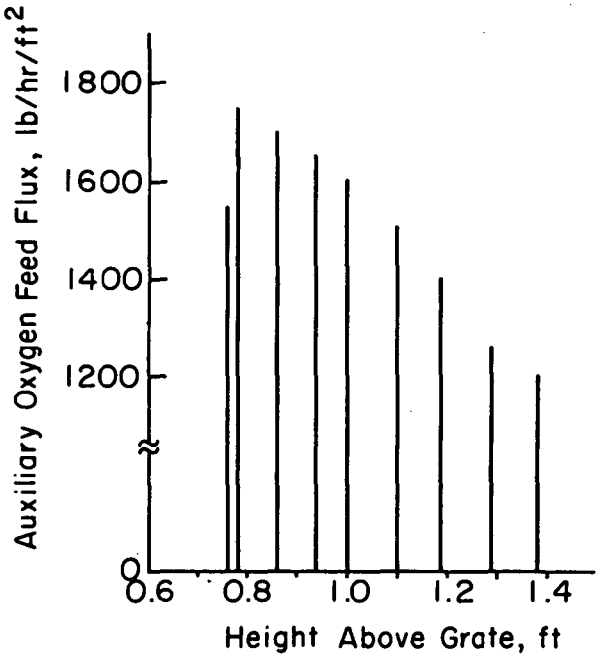

Figure 2. Auxiliary oxygen feed profile for Illinois No. 6 coal with a steam flux of 160 lb/hr/ft^2 and an oxygen feed flux to the bottom of 40 lb/hr/ft^2. (XBL 8312-4337)

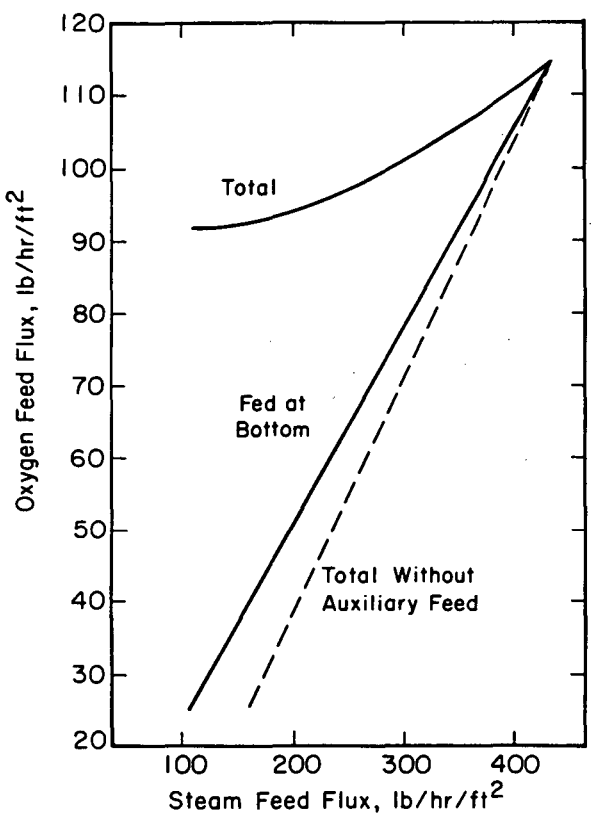

Figure 3. Oxygen flux with auxiliary feed as a function of steam flux, Illinois No. 6 coal. (XBL 8312-4338)

maximum temperature. Typical temperature profiles are shown in Fig. 4. As would be expected from the studies of Yoon *et al.*[5,6] and Yu *et al.*,[4,7] lowering the steam-to-oxygen ratio at the reactor bottom causes the location of maximum temperature in the reactor to fall for a fixed carbon conversion. This location can be kept constant by using the auxiliary feed to increase carbon conversion.

Product-gas compositions (using Yoon's average volatile compositions) are shown in Fig. 5 for the Illinois coal; the curves for the Wyoming coal are similar and essentially parallel, but are deleted for clarity.

The cold-gas efficiency, defined as the ratio of the lower heating value of the product gas per unit of coal feed to the lower heating value of the coal, is also shown in Fig. 5 for both coals. There is a 6% improvement in cold-gas efficiency for the Illinois coal and an improvement somewhat over 1% for the Wyoming coal. The change is not large because the reduction in steam essentially changes the H_2-CO balance through the water-gas shift equilibrium, and the heating values of the two gases are similar. The cold-gas efficiency reflects only part of the improvement in overall thermal efficiency, however, as there is an important gain resulting from the substantial reduction in the steam requirement and the smaller but still meaningful reduction in oxygen. On the basis of the calculations of Shinnar and Kuo[2] for an idealized reactor, the additional improvement in thermal efficiency for the Illinois coal at the lowest steam-to-oxygen ratio studied (2.1:1) will be of the same order as the increase in cold-gas efficiency. Shinnar and Kuo[2] note that the overall efficiency is greatly affected by the sum of the moles of steam

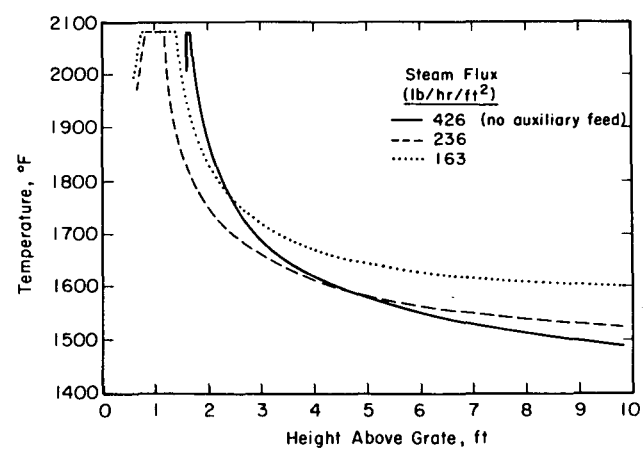

Figure 4. Temperature profiles with auxiliary feed for Illinois No. 6 coal, maintaining 0.01% unreacted carbon in the ash. (XBL 8312-4341)

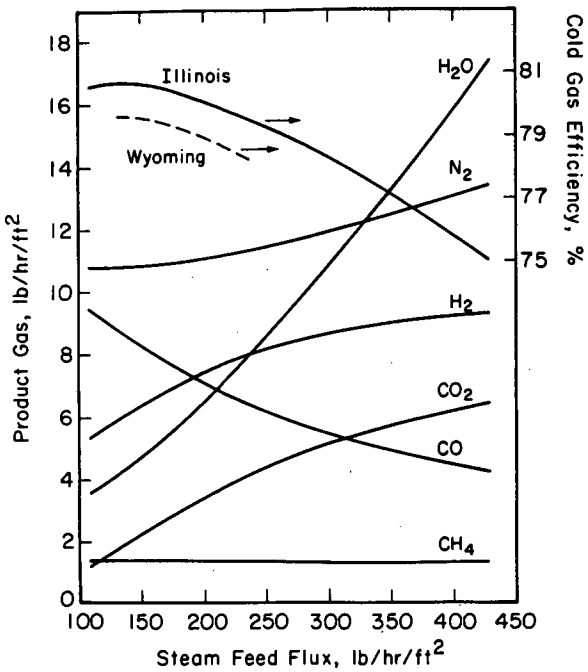

Figure 5. Product gas composition and cold gas efficiency as a function of steam flux with auxiliary feed. (XBL 8312–4342)

plus four times the moles of oxygen, because of the relative costs of producing the gaseous feeds; this sum is reduced to less than 50% of that required for a conventional bottom feed. The total potential improvement in efficiency is therefore substantial.

Implementation

A continuous distribution of feed is clearly impossible, but some trial calculations indicate that approximation of a feed program like that in Fig. 2 by two or three feed points, representing a small number of tuyeres, gives essentially the same results with a variation in the maximum temperature of about 20°F. The question of efficient radial distribution of the oxidant over a sufficiently short time scale to prevent unacceptably high temperatures from localized combustion has not been addressed.

The sensitivity of reactor performance to the placement of the auxiliary feed is an important consideration. The computed sensitivity is shown in Table 1 for Illinois No. 6 coal, with bottom-feed fluxes of 163 lb/hr/ft^2 steam and 40 lb/hr/ft^2 oxygen, and an auxiliary feed of 52 lb/hr/ft^2 oxygen. The auxiliary feed was placed at a position starting 1.6 ft above the grate, and extending over 0.6 ft, based on 0.0001% unreacted carbon in the ash in the reactor core. Operation at lower carbon conversion results in a first temperature peak below the auxiliary feed,

Table 1. Sensitivity of reactor performance to operating policy for auxiliary feed.[a]

Unreacted carbon in feed (%)	Position of first temp. maximum (ft)	Cold gas efficiency (%)
0.0001	1.6	80.2
0.01	0.8	80.1
0.1	0.4	79.9
1.0	0.2	79.0

[a]Auxiliary feed is 1.6 ft above grate, with flux of 52 lb/hr/ft^2 oxygen; bottom-feed flux is 163 lb/hr/ft^2 steam and 40 lb/hr/ft^2 oxygen; coal is low-reactivity Illinois No. 6.

followed by a second region at the maximum temperature in the auxiliary feed zone. The cold gas efficiency drops only 0.3% from the design level of 80.2% for a temperature peak at 0.4 ft (0.1% carbon in ash), and only 1.2% for a temperature maximum just slightly above the grate (1% carbon in ash). The increase in unreacted carbon in the reactor core decreases the cold-gas efficiency.

As can be seen from Fig. 6, the size of the auxiliary feed zone depends on coal reactivity. The distribution is carried out over a region 1.5 ft high for the low-reactivity eastern bituminous coal, while the zone is only about one inch in height for the high-

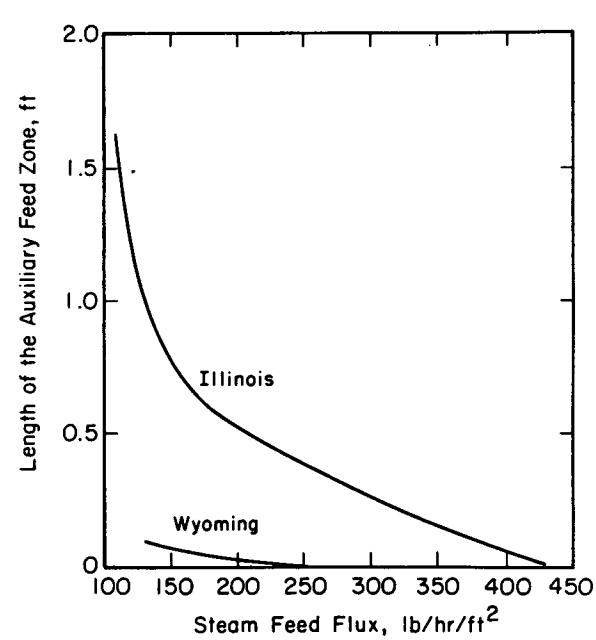

Figure 6. Length of auxiliary feed zone for low (Illinois) and high (Wyoming) reactivity coals. (XBL 8312–4340)

reactivity western subbituminous coal. The latter zone is comparable to the size of a single particle, and is clearly impractical, although it might be expanded by feeding oxidant at a lower rate. The tentative conclusion to be drawn, however, subject to more complete analysis of the problem of gas distribution, is that a distributed-feed reactor is likely to be practical only for the gasification of low-reactivity coals. These are the coals for which Sharman and Scott[3] described the slagger as being particularly suited.

Summary

Dry-ash moving-bed coal gasifiers such as the Lurgi are inefficient because of the high steam-to-oxygen ratio required to prevent the ash-softening temperature from being exceeded. Calculations based on a one-dimensional gasifier model show that it may be possible to reduce the steam requirement substantially for low-reactivity coal, almost to that of a slagging moving bed, by distributing part of the oxygen feed axially and broadening the combustion zone. Two to three axial injection ports should be adequate. This preliminary result does not take into account the problem of efficient radial distribution of the oxidant.

PLANNED ACTIVITIES FOR FY 1984

The concept of a distributed feed is based on the presumption that maximum temperature can be controlled. The model used in this study is known to entail uncertainties on the order of several hundred degrees in the prediction of the maximum temperature,[10] and the assumption of equal solid and gas temperatures appears to cause errors in the prediction of the point of maximum temperature.[11] Thus, to develop design equations, a more refined model that considers gas distribution and that resolves these uncertainties will be needed. Future work will attempt to develop such a model.

ACKNOWLEDGMENT

J. Wei was an active participant in earlier modeling work sponsored by the Electric Power Research Institute, in which the concept of an auxiliary feed was developed.

REFERENCES

1. Denn, M.M. and Shinnar, R. (1983), "Coal Gasifiers," in *Reaction Engineering Handbook*, J.J. Carberry and A. Varma, Eds., Marcel Dekker, in press.
2. Shinnar, R., and Kuo, J.C. (1978), "Gasification Study for Mobil Coal to Gasoline Process," Final Report, FE-2766-13, U.S. Department of Energy, Morgantown, WV.
3. Sharman, R.B., and Scott, J.E. (1981), "The British Gas/Lurgi Slagging Gasifier and its Relevance to Power Generation," in *Conference Proceedings: Synthetic Fuels—Status and Directions*, Vol. 2, EPRI WS-79-238, Electric Power Research Institute, Palo Alto, CA.
4. Denn, M.M., Wei, J., Yu, W.C. and Cwiklinski, R. (1982), "Detailed Simulation of a Moving-Bed Gasifier," EPRI AP-2576, Electric Power Research Institute, Palo Alto, CA.
5. Yoon, H., Wei, J. and Denn, M.M. (1977), "Modeling and Analysis of Moving Bed Coal Gasifiers," Vols. 1 and 2, EPRI AF-590, Electric Power Research Institute, Palo Alto, CA.
6. Yoon, H., Wei, J., and Denn, M.M. (1978), "A Model for Moving Bed Coal Gasification Reactors," *AIChE J. 24*, p. 885.
7. Yu, W.C., Denn, M.M., and Wei, J. (1983), "Radial Effects in Moving Bed Coal Gasifiers," *Chem. Eng. Sci. 38*, p. 1467.
8. Denn, M.M., Wei, J., and Child, J.E., unpublished research, University of Delaware, 1981; see Child, J.E., (1981), "Alternative Feed Strategies for Moving Bed Coal Gasifiers," B.Ch.E. thesis, University of Delaware, Newark, DE.
9. Yoon, H., Wei, J. and Denn, M.M. (1979), "Analysis of Lurgi Gasification of Two U.S. Coals," *Chem. Eng. Sci. 34*, p. 231.
10. Denn, M.M., Yu, W.C., and Wei, J. (1979), "Parameter Sensitivity and Kinetics-Free Modeling of Moving Bed Coal Gasifiers," *Ind. Eng. Chem. Fundamentals 18*, p. 226.
11. Cwiklinski, R., Wei, J. and Denn, M.M. (1981), "A Heterogeneous Moving Bed Coal Gasifier Model," presented at American Institute of Chemical Engineers National Meeting, Detroit, MI, August 1981; some results are in Denn, M.M. (1982), "Steady State and Dynamic Simulation of Moving Bed Gasifiers," in *Coal Gasification Modeling Workshop Proceedings*, M. Ghate and J.W. Martin, Eds., DOE/METC/82-24, U.S. Dept. of Energy, Morgantown, WV.

ELECTROCHEMICAL ENERGY STORAGE RESEARCH

Technology Base Research Project for Electrochemical Energy Storage*

E.J. Cairns, K. Kinoshita, and F.R. McLarnon

The Lawrence Berkeley Laboratory (LBL) is lead center for management of the Technology Base Research (TBR) Project, which is supported by the Electrochemical Branch of DOE's Energy Storage Division. The project provides the research base for DOE efforts to develop electrochemical technology for electric vehicles and stationary energy storage. The specific goal is to identify the most promising electrochemical technologies and transfer them to industry and/or another DOE program for further development and scale-up.

The TBR Project is divided into four major elements: electrochemical systems, supporting research, electrochemical processes, and fuel cell research. The generic research topics covered by each of these elements are listed in Table 1. During FY 1983, program management responsibility for research on iron/air cells was transferred from Lawrence Livermore National Laboratory (LLNL) to LBL; LLNL will continue technical management of aluminum/air projects.

General research areas addressed by the TBR Project include identification of new electrochemical couples for advanced batteries, determination of technical feasibility of the new couples, improvements in battery components and materials, establishment of engineering principles applicable to electrochemical energy storage and conversion, and investigations of fuel cell technology for transportation. Major emphasis is given to applied research that will lead to superior performance and lower life-cycle costs.

The LBL scientists participating in the program are E.J. Cairns, K. Kinoshita and F.R. McLarnon of the Applied Science Division, and L.C. DeJonghe, J.W. Evans, R.H. Muller, J.S. Newman, P.N. Ross, and C.W. Tobias of the Materials and Molecular Research Division.

*This work was supported by the Assistant Secretary for Conservation and Renewable Energy, Office of Energy Systems Research, Energy Storage Division of the U.S. Department of Energy under Contract No. DE-AC03-76SF00098.

Table 1. Topics covered by the Technology Base Research Project for Electrochemical Energy Storage.

I. ELECTROCHEMICAL SYSTEMS

- New Rechargeable Electrochemical Cells
- Metal/Air Cells

II. SUPPORTING RESEARCH

A. Engineering-Science Research

- Electrode Morphological Studies, Chemical/Structural Analysis
- Transport Phenomena, Electrocatalysis, Electrode Kinetics, and Cell Thermodynamics
- Modeling of Electrochemical Cells and Battery Systems
- Advanced Physicochemical Methods for Electrochemical Research

B. Materials Research

- Ceramic, Molten-Salt, Glass, and Polymeric Electrolytes
- Novel Electrode Structures
- New Fabrication Techniques for Components
- Battery Separators

III. ELECTROCHEMICAL PROCESSES

- Corrosion Problems in Electrochemical Storage Devices
- Characterization of Three-Phase Electrochemical Systems
- Thermally Regenerative Cells

IV. FUEL CELL RESEARCH

- New Components for Fuel Cells
- New Electrolytes
- Electrocatalysis

ACCOMPLISHMENTS DURING FY 1983

LBL monitored close to 40 subcontracts during FY 1983 and conducted a vigorous in-house research program. Projects conducted by the subcontractors

are described in the recent report, *Technology Base Research Project for Electrochemical Energy Storage* (LBL-15992); the in-house work, "Electrochemical Energy Storage," is summarized in the next article and in the *Materials and Molecular Research Division FY 1983 Annual Report* (LBL-16680). Highlights of the subcontracted work follow.

Electrochemical Systems

- Eltech Systems Corporation was selected to be the prime industrial subcontractor for aluminum/air battery R&D.
- Eltech Systems achieved 1400 simulated driving cycles in lifetime testing of a cathode with improved structure and an electrocatalyst of cobalt meso-tetra-p-methoxyphenylporphyrin. This result is only 100 cycles less than the program goal of 1500 cycles.
- LLNL has successfully operated an integrated system consisting of a single-wedge cell and a crystallizer/hydrocyclone separator for a mechanically rechargeable aluminum/air battery.
- Tests at EIC Laboratories, Inc. indicate that sulfolane-based organic electrolytes in ambient-temperature lithium batteries may be stable at temperatures up to 70°C.
- The research effort on sodium/alkali-nitrate cells at Argonne National Laboratory was terminated because of problems encountered with corrosion, stability of β''-alumina in the presence of $LiNO_3$ + $NaNO_3$, and operating temperatures that are 80–100°C higher than the goal of 200°C.

Supporting Research

- The Massachusetts Institute of Technology has completed a study on the compositional changes in NASICON ($Na_{1+x}Zr_2Si_xP_{3-x}O_{12}$) at room temperature. Although further development work on this electrolyte for Na/S batteries was terminated because of its degradation in hot sodium, the information gained from this study will be useful for tailoring new compositions with similar structural parameters.
- Argonne National Laboratory has prepared NASIGLAS (*Na*$^+$ *S*uper *I*onic *G*lass, $Na_{1+x}Zr_{2-x/3}Si_xP_{3-x}O_{12-2x/3}$), analogues of NASICON that show encouraging stability in molten sodium. A review of the literature on glass chemistry suggests that a NASIGLAS-solid electrolyte can be developed that will be resistant to sodium attack and will have a resistivity of less than 100 ohm-cm at 300°C.
- A specially designed high-temperature calorimeter was employed by Gould, Inc. to measure the heat generation rates of a LiAl/FeS cell. The measured results showed excellent agreement with values of cell heat generation predicted from thermodynamic calculations.
- LLNL identified a zinc-halide electrolyte composition in which cross-term diffusion coefficients are significant, in contrast to previous measurements that had indicated cross-term diffusion coefficients were small. The new findings suggest that extreme care must be taken to accurately model transport processes in zinc/halogen cells.
- Research and development projects on separators for batteries were expanded. Brigham Young University and Pinnacle Research Institute began research to develop improved separators for alkaline batteries. Castle Technology's results in developing supported liquid-membrane separators for batteries were sufficiently promising that life-cycle tests in Zn/NiOOH cells are in progress.

Electrochemical Processes

- Experiments are under way at Argonne National Laboratory to develop new alloys for positive-side current collectors and containment materials in Na/S and Li/FeS_2 cells. Studies of the sulfidation of unalloyed metals at 350°C indicated that candidate base metals, such as nickel and iron, show positive deviation from a parabolic rate of sulfide-scale formation in less than a day. The sulfide scales that formed on alloying elements such as aluminum and molybdenum, remained diffusion-controlled throughout the four-day test.
- Research at Case Western Reserve University on the use of transition-metal macrocyclics (TMM) as electrocatalysts for air electrodes indicates that heat treatment of TMM's improves their electrocatalytic activity.
- Research at the Solar Energy Research Institute on redox couples for thermally regenerative electrochemical systems was phased out.

Fuel Cell Research

- Los Alamos National Laboratory (LANL) has developed an *in situ* ion-beam technique for characterizing electrode surfaces under conditions closely approximating a working electrochemical cell. Analysis of new and used electrodes with a platinum-vanadium electrocatalyst at the cathode showed that under operating conditions the PtV is not stable; V dissolves in the electrolyte and is

transported through the matrix to the anode. These results are consistent with the observed performance degradation of the fuel cell.

- LANL has applied analytical and electrochemical techniques to study the structure, transport, and stability of solid-polymer electrolytes (SPE). Proton NMR studies of Nafion showed that cations coupled to the ion-exchange sites were solvated with different quantities of water, depending on the specific cation involved. Electron microprobe and scanning electron microscope analyses indicated that no sulfur attack occurred during cell operation. Water transport through Nafion 117 was found to be approximately four times faster than through Nafion 125.
- The reduction of oxygen on tetrasulfonated metal phthalocyanines (M-TSP) of iron, cobalt, nickel, and manganese in 0.1 *N* TFMSA was measured by Brookhaven National Laboratory. The activities of the M-TSP's for oxygen reduction decreased in the order Fe > Co > Mn > Ni. No activity was found for carbon monoxide or formic acid oxidation with these electrocatalysts.
- Systems studies were performed by LANL for selected heavy-duty transportation systems, consumer vehicles, and buses; these studies used the vehicle-simulation program developed at LANL. The studies of heavy-duty systems examined the feasibility of using fuel cells to power locomotives and river tow boats, and found the locomotive application promising.
- Two new research efforts were initiated: (1) General Electric Company investigated methods of reducing the cost of the membrane and catalyst for SPE cells while maintaining performance levels, and (2) United Technologies Corporation investigated alloy and redox catalysts in phosphoric acid systems with the goal of increasing overload capability, increasing efficiency, and reducing catalyst cost.

PLANNED ACTIVITIES FOR FY 1984

Major new initiatives include the following:

- Selections will be made from proposals submitted in response to a Request for Proposals (RFP) on Applied Research on Advanced Secondary Batteries. The RFP, issued by the TBR Project, solicited research proposals relevant to:
  (1) Improving the performance and rechargeability of ambient-temperature metal electrodes in non-aqueous electrolytes.
  (2) Advancing the technology and developing new components for molten-salt batteries such as Li/FeS_2 and Na/S.
  (3) Developing improved methods to store halogens for Zn/halogen batteries.
  (4) Improving electrocatalysts for air electrodes and development of corrosion-resistant supports for bifunctional air electrodes.
- Research to identify new separators for Zn/ferricyanide redox cells will be initiated.
- Work on a thermally regenerative system using sodium will begin.

Battery Electrode Studies*†

E.J. Cairns, F.R. McLarnon, J.C. Dobson, J.H. Flatt, R.I. Goldberg, M. Isaacson, R. Jain, P.M. Lessner, K.G. Miller, M.L. Smith, and K.A. Striebel

This research focuses on the behavior of electrodes used in secondary batteries and investigates practical means for improving their performance and lifetime. Systems of current interest include ambient-temperature rechargeable cells with zinc electrodes [Zn/NiOOH, Zn/AgO, Zn/Cl_2, $ZnBr_2$, Zn/air, and $Zn/Fe(CN)_6^{-3}$]; rechargeable molten-salt cells (Li-Al/FeS, $Li\text{-}Al/FeS_2$, Li-Si/FeS, $Li\text{-}Si/FeS_2$, and $Na/\beta''\text{-}Al_2O_3/NaCl\text{-}AlCl_3\text{-}SCl_4$); fuel cells; and liquid-junction photovoltaic cells. Life- and performance-limiting phenomena are studied under realistic cell operating conditions.

ACCOMPLISHMENTS DURING FY 1983

Optical and Electrochemical Study of Model Zinc Electrode Pores in Alkaline Electrolytes

(J.H. Flatt, F.R. McLarnon, and E.J. Cairns)

A computer-controlled, single-pore cell has been developed to study zinc-electrode discharge behavior

*This work was supported by the Assistant Secretary for Conservation and Renewable Energy, Office of Energy Systems Research, Energy Storage Division of the U.S. Department of Energy under Contract No. DE-AC03-76SF00098.

†This project is part of a larger effort, "Electrochemical Energy Storage," described in the *Materials and Molecular Research Division FY 1983 Annual Report* (LBL-16680).

in alkaline electrolytes. Information on pore potential distribution and hydroxyl ion concentration is provided by a quartz-supported, thin-film cadmium reference microelectrode in the cell. This microelectrode, fabricated by microelectronic metal deposition and photolithographic techniques, was designed to be stable in strong alkaline electrolytes without significantly interfering with transport processes in the pore. The model pores created in the cell are intended to be of dimensions comparable to those in commercial zinc electrodes—between 14 and 20 microns in effective radii in our initial studies.

These studies, which used 7 mA/cm^2, 30 mA/cm^2, and 1250 mA/cm^2 rates of discharge in 7.7 *M* KOH electrolyte, showed results consistent with a dissolution-precipitation discharge reaction mechanism. Scanning electron microscopy (SEM) studies showed significant variations in electrode surface morphology with location in the pore and rate of discharge. Significant pore $[OH^-]$ gradients, with slow relaxation times, existed within the pore at the 30 mA/cm^2 rate. Electrode passivation was observed only at the 1250 mA/cm^2 rate. Zinc electrode discharge behavior in 3.5 *M* KOH–3.4 *M* KF showed a similar discharge reaction mechanism. However, earlier surface film formation occurred, which is consistent with reduced zinc solubility. Earlier film formation may decrease zinc redistribution rates by decreasing the residence time of soluble zinc species in the electrolyte. Initial reaction penetration depths in 7.7 *M* KOH and 3.5 *M* KOH-3.4 *M* KF were 0.11 cm and 0.10 cm, respectively.

Mathematical Modeling of the Zinc Electrode

(K.G. Miller, E.J. Cairns, and F.R. McLarnon)

Phenomena that limit the cycle life of secondary zinc electrodes include shape change[1,2] (redistribution of active material over the face of the electrode) and passivation[3] (formation of oxide layers over the surface of the electrode). One-dimensional models[2,3] have already been proposed to account for these phenomena. Our goal is to develop a two-dimensional, time-dependent model to predict the extent of shape change and passivation as the electrode is cycled. This model must account for changes in current density, electrode overpotential, and species concentration, both parallel and perpendicular to the plane of the zinc electrode.

An existing one-dimensional model[3] is being assessed for its sensitivity to various physical parameters. The parameters to which this model is most sensitive will be measured for application in the two-dimensional model.

Analysis of Zinc Electrode Current Collection in Zn/NiOOH Cells

(R.I. Goldberg, E.J. Cairns, and F.R. McLarnon)

Mathematical models have been developed[4] to characterize the ability of a current collector to promote a uniform current density distribution over the electrode (the macroscopic current distribution). This study is employing such models to correlate various current-collector designs with Zn/NiOOH cell performance and lifetime.

Specific parameters known to substantially affect the macroscopic current distribution over the surface of a battery electrode include the resistances of the current collector members, the applied current to the electrode, and the placement and geometry of the tabs that provide electrical connection to the external circuit. The microscopic current distribution (i.e., the distribution within the porous electrode structure) depends on the detailed structure and geometry of the current collector and the resistivity of the electrolyte- and electrode-active materials. These parameters will be accounted for in the mathematical model and in the fabrication of various current collectors. Model Zn/NiOOH cells will be built and tested with a computer-controlled test system[5] previously developed at LBL.

The Effect of Mixed Electrolytes on the Performance of Zn/NiOOH Cells

(M. Isaacson, E.J. Cairns, and F.R. McLarnon)

The high solubility of the zincate ion contributes to the limited cycle life of the secondary zinc electrode.[3] The effect of adding a less-polar organic solvent to alkaline KOH electrolyte is being investigated as a means to reduce the solubility of the zincate ion and thereby extend the lifetime of the zinc electrode.

Preliminary studies have focused on alcohols as electrolyte additives. Experiments showed that methanol reduced the zincate solubility by approximately 70% for a 30% KOH–40% water–30% methanol electrolyte. However, tests in model Zn/NiOOH cells showed that methanol was oxidized to a considerable extent on the NiOOH electrode.

Investigation of other organic solvents is continuing. Solvents with high electrochemical stability, such as sulfolane, dimethylformamide, and butyrolactone may reduce zincate solubility while also maintaining sufficient chemical stability.

Rechargeable Zinc Electrodes of the Second Kind

(R. Jain, E.J. Cairns, and F.R. McLarnon)

The aim of this project is to investigate the addition of alkaline-earth metals to the zinc electrode as a practical means of reducing zinc species solubility in alkaline electrolytes, thereby improving the cycle life of such electrodes. A preliminary literature survey indicated[6,7] that, of the alkaline-earth-metal hydroxides, only calcium hydroxide appears to inhibit the solubility of ZnO.

Corrosion of Metals by Sulfur-Polysulfide Melts

(J.C. Dobson, F.R. McLarnon, and E.J. Cairns)

One problem in the design of high-temperature alkali-metal/sulfur cells is the corrosion of the metal cell container at the sulfur electrode. Although many studies have been made of the corrosion of various metals and alloys, particularly in sodium/sulfur cells, very little is known about the relationship of the corrosion rates to the kinetic, thermodynamic, and mechanistic parameters governing processes at the current collector. This work attempts to establish this relationship through the comparison of corrosion data with existing models for oxidation and sulfidation of metals in gases. Corrosion phenomena on various metals and alloys in lithium- and sodium-sulfur-polysulfide melts are being studied over the composition, temperature, and potential ranges expected during the operation of the corresponding high-temperature cells.

Both static and electrochemical corrosion studies are under way. Melt compositions were chosen to reflect expected variations in sulfur activity and were generally confined to the single-phase liquid regions of the Na_2S-S and Li_2S-S phase diagrams. Materials under study include Mo, Cr, and a 70% Cr–30% Fe alloy. Cross sections of the specimens are studied using SEM coupled with electron diffraction analysis (EDAX) techniques to determine the thickness and composition of the scale. Weight gain is also used to calculate overall corrosion rates, where possible. Even temperature distribution is maintained by placing the quartz ampules in an insulated aluminum block heated by cartridge heaters.

These experiments use the electrochemical cell shown in Fig. 1. The body of the cell is constructed from quartz. A molybdenum feedthrough is the reference electrode, and tungsten springs serve both

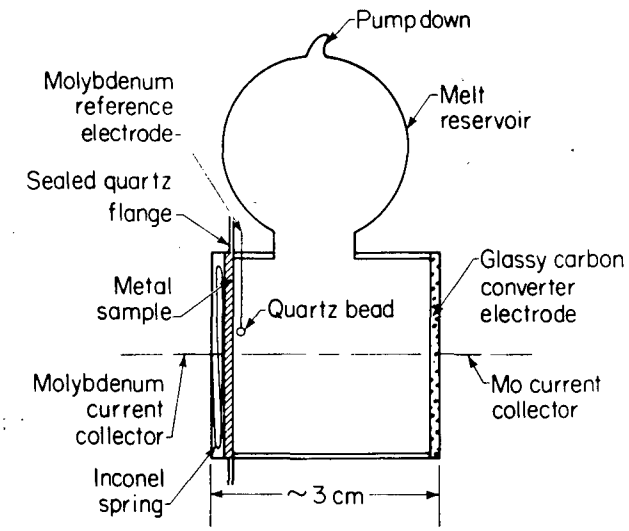

Figure 1. Electrochemical cell for corrosion experiments. (XBL 835–2620)

to collect current and to hold the electrodes in place. The metallic samples are maintained at a fixed potential relative to the Mo/MoS_2 reference electrode, and the cell current and resistance of the scale are measured during the run to determine the scale thickness as a function of time.

Initial results of static corrosion tests on Mo showed that it is resistant to corrosion at 400°C in Li_2S-S melts, apparently independently of sulfur activity. Quantitative results proved elusive, however, since EDAX techniques are incapable of distinguishing between S and Mo. Also, the scale is so thin (on samples corroded for one week) that optical methods yield little measurable data. Using sulfur-35 as a radioactive tracer to solve this problem is being investigated.

Glass Electrolytes for Li/S Cells

(M.L. Smith, F.R. McLarnon, and E.J. Cairns)

Several borate glasses have been developed[8] that, upon addition of Li_2O and LiCl, show lithium-ion conductivities as high as 2×10^{-2} $(\Omega\text{-cm})^{-1}$ at 300°C. It has also been observed that the structures of these glasses are maintained in the presence of molten Li. We are now examining the stability of these borate glasses in molten sulfur/polysulfides. The aim is to build and test a Li/S or Li alloy/S cell that employs a fast ion-conducting borate glass as the electrolyte.

Novel Electrolytes for Fuel Cells

(K.A. Striebel, P.C. Andricacos,‡ E.J. Cairns, P.N. Ross,‡ and F.R. McLarnon)

The large overpotential encountered in the oxygen electrode is one of the major factors limiting the efficiency of fuel cells. Recent studies have shown that the kinetics of oxygen reduction on platinum in trifluoromethane sulfonic acid (TFMSA) are significantly improved over those in phosphoric acid, the current "standard." This has been attributed[9] to the absence of anion-specific adsorption on Pt in TFMSA. The "dimer" of TFMSA is tetrafluoro-1,2-disulfonic acid (TFEDSA). This acid exhibits higher contact angles with Teflon and lower acid vapor pressures.[10]

The kinetic currents for oxygen reduction in TFEDSA and TFMSA were measured in rotating-disk experiments. The acids show similar behavior when compared at a pH of one (Fig. 2). The reaction order with respect to oxygen was determined in both electrolytes to be unity by using gases with various partial pressures of oxygen.

The kinetic currents are extremely sensitive to low levels of adsorbing impurities, and transient techniques are being developed to minimize these effects or render them constant. Future work will focus on electrode kinetics in more concentrated electrolytes.

Engineering Analysis of Photoelectrochemical Cells

(P.M. Lessner, E.J. Cairns, and F.R. McLarnon)

The sulfide/polysulfide redox couple has been found to stabilize several semiconductors that are efficient solar convertors for photoelectrochemical cells. Before this redox couple an be used in such cells, however, several major problems must be solved. These include photocorrosion of the semiconductors and design of the counterelectrode. Recent work on this project has focused on understanding the complex chemistry of the sulfide/polysulfide redox couple to improve the counterelectrode design.

Some preliminary kinetic data have been collected, but accurately interpreting them was difficult because of inconsistent and incomplete thermodynamic data. Recent efforts have therefore concentrated on building and expanding a thermodynamic data base. When this data base is completed, kinetic experiments will resume.

‡Materials and Molecular Research Division.

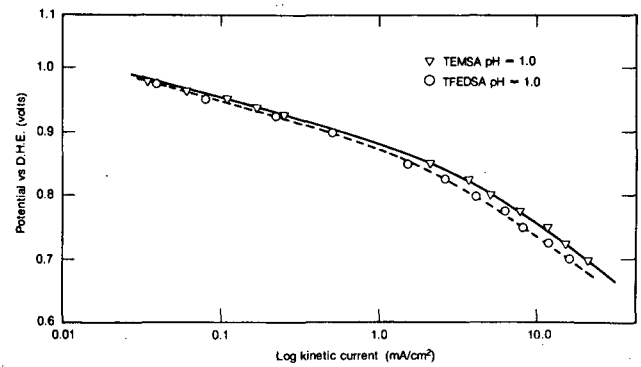

Figure 2. Tafel plots for oxygen reduction on platinum at 25°C. Circles, 0.05 *M* TFEDSA; inverted triangles, 0.1 *M* TFMSA. (XBL 8311-700Y)

PLANNED ACTIVITIES FOR FY 1984

Continuing research efforts on secondary alkaline zinc electrodes will focus on the development of a two-dimensional, time-dependent mathematical model; the analysis of zinc electrode current collection; electrolyte and electrode formulations that exhibit reduced zinc-species solubility; and the microscopic study of model zinc electrodes. Work with high-temperature alkali-metal/sulfur cells will continue to investigate the corrosion of candidate materials for positive-electrode current collectors and to examine Li/glass electrolyte/S cell configurations. Efforts to model the sulfur/polysulfide electrode will begin. Additional research on electrolytes for fuel cells and analysis of photoelectrochemical cells will continue.

REFERENCES

1. McBreen, J. (1972), "Zinc Electrode Shape Change in Secondary Cells," *J. Electrochem. Soc.119*, p. 1620.
2. Choi, K.W., Bennion, D.N., and Newman, J. (1976), "Engineering Analysis of Shape Change in Zinc Secondary Electrodes. I. Theoretical," *J. Electrochem. Soc. 123*, 1616; "Engineering Analysis of Shape Change in Zinc Secondary Cells. II. Experimental," *ibid.*, p. 1628.
3. Sunu, W.G., and Bennion, D.N. (1980), "Transient and Failure Analyses of the Porous Zinc Electrode. I. Theoretical," *J. Electrochem. Soc. 127*, p. 2007; "Transient and Failure Analyses of the Porous Zinc Electrode. II. Experimental," *ibid.*, p. 2017.

4. Gu, H. (1983), "Mathematical Analysis of a Zn/NiOOH Cell," *J. Electrochem. Soc. 130*, p. 1459.

5. Katz, M.H., Nichols, J.T., McLarnon, F.R., and Cairns, E.J. (1983), "Computer-Controlled Multiple-Channel System for Electrochemical Experiments," *J. Power Sources 10*, p. 149.

6. Kawamura, G. and Yoshiyuki, M. (1980), "A Study of Insoluble Zinc Electrodes for Alkaline Secondary Batteries. I. Insolubilizing the Zincate Ion by Calcium Hydroxides," *Denki Kagaku 2*, p. 592.

7. General Motors Corporation (1980), "Nickel-Zinc Electric Storage Battery Cells," European Patent Application No. 80303285.3, filed 18 September 1980.

8. Button, D.P., Tandon, R.P., Tuller, H.L., and Uhlmann, D.R. (1981), "Fast Li Ion Conductance in Chloro-Borate Glasses. II. Di Borates and Metaborates," *J. Solid State Ionics 5*, p. 655.

9. Ross, P.N. and Andricacos, P.C. (1983), "The Effect of the $H_2PO_4^-$ Anion on the Kinetics of Oxygen Reduction on Platinum," *J. Electroanal. Chem. 154*, p. 205.

10. Ross, P.N. (1983), "Evaluation of Tetrafluoroethane-1,2-Disulfonic Acid as a Fuel Cell Electrolyte," *J. Electrochem. Soc. 130*, p. 882.

Advanced Thermal Energy Storage Technologies*

P. Berdahl, A. Hunt, C. Tien, and R.J. Otto

Conservation and renewable energy programs have made real gains in the past 10 years, leading to the commercialization of new systems and the emergence of new industries. However, parts of the energy-supply, distribution, and end-use sectors could still see significant cost savings through the use of energy storage systems and, in particular, thermal energy storage systems. Thermal energy storage (TES) has traditionally and logically been divided into three areas: sensible heat, latent heat (phase-change materials), and thermochemical heat storage.[1]

A research program in TES technologies was started at LBL in July of FY 1983. Research projects composing the TES program were selected by the Department of Energy as being new and innovative approaches to thermal energy storage with a broad range of potential applications. However, two particularly important targets for thermal energy storage research are cooling and heating work for living spaces in buildings and thermochemical energy storage using solar energy. The criteria for project selection and development have focused on fundamental aspects such as the thermodynamics, kinetics, and thermal-material properties of the storage systems in order to identify the most promising innovative ideas. Systems with the potential for low irreversible entropy gains and large reversible entropy changes are desirable.

Four research projects will be carried forward at LBL in FY 1984. These projects are:

(1) development of a solid-state radiative heat pump, with one of its important potential applications being residential cooling;
(2) thermochemical conversion and storage of radiant energy using small particles as heat exchanger and catalyst with potential application to thermochemical storage of solar energy;
(3) optimization of thermal-material structure; and
(4) investigation of alloys with abnormally large heat capacities and reactions with large entropy change.

The planned research is designed to test the feasibility of these concepts and to move them from proof of concept to the threshold of development.

ACCOMPLISHMENTS DURING FY 1983

Funding for the first three projects was received late in FY 1983, and preliminary research results will be included in next year's annual report. Work on the fourth project is led by L. Brewer, R. Connick, and N. Phillips, investigators in the Materials and Molecular Research Division, which will include this effort in its annual reports; it is also summarized in Ref. 2.

PLANNED ACTIVITIES FOR FY 1984

Solid-State Radiative Heat Pump

(Paul Berdahl)

It is proposed to perform research leading to the development of a large-area thin-film solid-state device that can use electrical energy to "pump" heat radiation. Depending on the sign of the applied electrical bias, the proposed device can be used for both heating and cooling. Because of its potential simplicity and reliability, this is a particularly attractive type of heat pump, and one that might replace conventional vapor-compression devices in some applications—for example, charging a residential cool storage system for summertime electric load management. A well-designed residence has modest cooling requirements, making it difficult to justify the investment in an efficient vapor compression machine. A solid-state device that can perform the same job may have a lower first cost.

The proposed physical structure of the solid-state radiative heat pump is a large-area, thin-film semiconducting diode, fabricated from a narrow-bandgap semiconductor. When forward-biased, charge-carrier injection through the junction results in electron-hole recombination radiation. Part of the energy emitted in the form of infrared radiation comes from the

*This work was supported by the Assistant Secretary for Conservation and Renewable Energy, Office of Energy Technologies Systems, Physical and Chemical Energy Storage Division of the U.S. Department of Energy under contract DE-AC03-76SF00098.

heat of the semiconductor lattice. This makes the device a type of heat pump. Under reverse bias, the device extracts charge carriers from the vicinity of the junction. This carrier depletion results in less recombination radiation being emitted than is normal for thermal equilibrium. The device could thus cool a nearby object by absorbing its thermal radiation.

After an initial period of theoretical evaluation in FY 1983, the concept of this solid-state radiative heat pump (SSRHP) concept still appears very promising. Although the parasitic Auger recombination mechanism requires additional theoretical work to assess its importance, it is imperative in FY 1984 to initiate and emphasize experimental research. The most straightforward approach to the construction of prototype devices, the fabrication of p-n junction photodiodes, would not be an efficient technique for evaluating a number of materials. For this reason, a galvano-magnetic technique will be used to produce nonequilibrium emission of infrared radiation from semiconducting samples. The galvano-magnetic luminescence experiments can form the basis of an SSRHP. However, a technologically mature device would presumably be based on a p-n junction diode that would be developed at a later stage of the research.

Thermochemical Conversion and Storage Using Small Particles as Heat Exchanger and Catalyst

(A. Hunt)

To explore the use of small particle suspensions and microstructured materials for energy conversion and storage systems requires a directed research program to examine critical aspects of the direct radiant chemical conversion process. In our initial studies in FY 1983, we examined the issues of heat transfer between the particles and gas. These studies indicated that particle size and gas characteristics had important effects on the particle heating and must be considered in any reactor design or in the interpretation of experimental results. In earlier work on a small-particle heat exchange receiver and in the radiant reactor design studies, the effect of the optical properties of the particles was examined. For thermal energy storage applications, the catalytic effects due to the small particles undergoing heating in the presence of concentrated sunlight was identified as the critical issue to examine in FY 1984. An analytical and experimental program to investigate high-temperature chemical reactions in the presence of short-wavelength solar radiation will elucidate the potential for direct solar chemical reactions to be applied to thermal energy storage.

Optimization of Thermal Material Structure for Thermal Energy Storage

(C.L. Tien, R. Greif, J. Humphrey, V. Carey, B. Rubinsky, and K. Udell)

The commercial use of thermal energy storage has been impeded by the failure of existing TES systems to meet one or more of the following criteria: efficient and effective heat transfer characteristics, high energy storage per unit volume, low maintenance operation, long operational lifetime, and cost. This failure is due, in part, to the lack of a fundamental understanding of the heat transfer characteristics essential to optimizing specific designs. There is a clear need for basic research that combines the study of heat transfer in multicomponent phase-change systems with emerging and advanced materials and designs.

The major objective of the proposed research is to explore promising new concepts in optimizing thermal-material structure for thermal energy storage. Particular emphasis will be placed on multicomponent phase-change systems with the combined features of high thermal energy storage capacity and effective heat transfer characteristics, and having the potential to operate as integrated thermal storage, thermal diode, and thermal switching devices. Fundamental in-depth research will be conducted on the complex physical phenomena involved in these systems in order to accurately assess and optimize performance. The proposed research also aims at achieving a better fundamental understanding of the physical processes in integrated TES systems.

REFERENCES

1. Lane, G.A., ed. (1983), *Solar Heat Storage: Latent Heat Materials*, CRC Press, Inc., Boca Raton, FL.
2. Brewer, L., Connick, R.E., and Phillips, N.E. (1983), "Thermal Energy Storage Utilizing Materials with Abnormally High Heat Capacities or Large Entropy Change Reactions," in *Proceedings of the DOE Physical and Chemical Energy Storage Annual Contractors Review Meeting, September 12–14, 1983*, Arlington VA, CONF-830974.

This report was done with support from the Department of Energy. Any conclusions or opinions expressed in this report represent solely those of the author(s) and not necessarily those of The Regents of the University of California, the Lawrence Berkeley Laboratory or the Department of Energy.

Reference to a company or product name does not imply approval or recommendation of the product by the University of California or the U.S. Department of Energy to the exclusion of others that may be suitable.

TECHNICAL INFORMATION DEPARTMENT
LAWRENCE BERKELEY LABORATORY
UNIVERSITY OF CALIFORNIA
BERKELEY, CALIFORNIA 94720